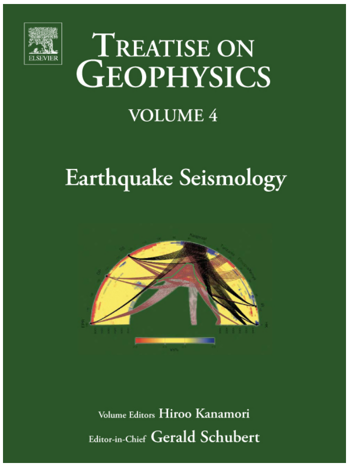
ELSEVIER
TREATISE ON
GEOPHYSICS
VOLUME 4
Earthquake Seismology
Volume Editors Hiroo Kanamori
Editor-in-Chief Gerald Schubert

4.22 The Role of Fault Zone Drilling

M. D. Zoback, Stanford University, Stanford, CA, USA

S. Hickman and W. Ellsworth, US Geological Survey, Menlo Park, CA, USA

4.22.1	**Introduction – Why Drill to Study Earthquakes?**	649
4.22.2	**Fluids and Faulting**	651
4.22.2.1	Sources of Fault-Zone Fluids	651
4.22.2.2	Fault-Zone Permeability	651
4.22.2.3	Transient Fluid Pressure Effects	652
4.22.2.4	Chemical Effects of Fluids on Fault-Zone Rheology	652
4.22.3	**Frictional Strength of Faults**	653
4.22.3.1	Weak Plate-Bounding Faults	654
4.22.4	**Near-Field Observations of Earthquake Nucleation and Propagation**	657
4.22.5	**Fault-Zone Drilling Projects**	658
4.22.5.1	Fault Behavior	659
4.22.5.2	Fluid Pressure	659
4.22.5.3	Fault Fluids	659
4.22.5.4	Fault-Zone Properties and Physical Parameters	659
4.22.5.5	Fault Structure and Materials	659
4.22.5.6	San Andreas Fault Observatory at Depth	659
4.22.5.7	Nojiima Fault	661
4.22.5.8	Chelungpu Fault	662
4.22.5.9	Gulf of Corinth	663
4.22.5.10	NELSAM	667
4.22.5.11	NanTroSeize	668
4.22.6	**Summary**	669
References		670

4.22.1 Introduction – Why Drill to Study Earthquakes?

The objective of fault-zone drilling projects is to directly study the physical and chemical processes that control deformation and earthquake generation within active fault zones. An enormous amount of field, laboratory, and theoretical work has been directed toward the mechanical and hydrological behavior of faults over the past several decades. Nonetheless, it is currently impossible to differentiate between – or even adequately constrain – the numerous conceptual models of active faults proposed over the years. For this reason, the Earth science community is left in the untenable position of having no generally accepted paradigm for the mechanical behavior of faults at depth. One of the primary causes for this dilemma is the difficulty of either directly observing or inferring physical properties and deformation mechanisms along faults at depth, as well as the need to observe directly key parameters such as the state of stress acting on faults at depth, pore fluid pressure (and its possible variation in space and time), and processes associated with earthquake nucleation and rupture. Today, we know very little about the composition of active faults at depth, their constitutive properties, the state of *in situ* stress or pore pressure within fault zones, the origin of fault-zone pore fluids, or the nature and significance of time-dependent fault-zone processes.

Most of what we now know about the structure, composition, and deformation mechanisms of crustal faults has been learned from geological investigations of exhumed faults, particularly where erosion has exposed previously deeply buried fault rocks. These field observations have proved to be particularly useful for several reasons. First, field observations of exhumed faults allow broad coverage with respect to variations in faulting style (e.g., comparing strike slip, normal and reverse faults), fault movement history, and local geology. Second, where sufficient surface outcrops exist, field observations can readily address issues related to geometrical complexity and spatial heterogeneity in physical properties and fluid composition (e.g., Kerrich *et al.*, 1984; Parry, 1994; Evans and Chester, 1995).

Constraints on the mechanical state and physical properties of active fault zones (e.g., fluid pressure, stress and permeability) from surface observations are indirect and subject to alternate interpretations. Stress heterogeneities induced by fault slip can lead to considerable uncertainties in inferring past fluid pressures from observations of vein geometry in outcrop. In all of these investigations, a complex history of uplift and denudation may have severely altered evidence of deformation mechanisms, fault-zone mineralogy, and fluid composition operative during fault slip. This problem is especially acute for solution–transport–deformation mechanisms (e.g., pressure solution and crack healing/sealing) and other low-activation-energy processes, as the deformation microstructures formed at depth are easily overprinted by ongoing deformation as the fault rocks are brought to the surface. Thus, the importance of fluids in earthquake generation and rupture is impossible to assess with any degree of certainty based solely on studies of exhumed fault rocks.

Fault-zone drilling projects allow us to address a number of first-order questions related to fault mechanics:

What are the mineralogy, deformation mechanisms and constitutive properties of fault gouge? Why do some faults creep? What are the strength and frictional properties of recovered fault rocks at realistic *in situ* conditions of stress, fluid pressure, temperature, strain rate, and pore fluid chemistry? What determines the depth of the shallow seismic-to-aseismic transition? What do mineralogical, geochemical, and microstructural analyses reveal about the nature and extent of water–rock interaction?

What is the fluid pressure and permeability within and adjacent to fault zones? Are there superhydrostatic fluid pressures within some fault zones and through what mechanisms are these pressures generated and/or maintained? How does fluid pressure vary during deformation and episodic fault slip (creep and earthquakes)? Do fluid pressure seals exist within or adjacent to fault zones and at what scales?

What are the composition and origin of fault-zone fluids and gasses? Are these fluids of meteoric, metamorphic, or mantle origin (or combinations of the three)? Is fluid chemistry relatively homogeneous, indicating pervasive fluid flow and mixing, or heterogeneous, indicating channelized flow and/or fluid compartmentalization?

How do stress orientations and magnitudes vary across fault zones? Are principal stress directions and magnitudes different within the deforming core of weak fault zones than in the adjacent (stronger) country rock, as predicted by some theoretical models? How does fault strength measured in the near field compare with depth-averaged strengths inferred from heat flow and regional stress directions? What is the nature and origin of stress heterogeneity near active faults?

How do earthquakes nucleate? Does seismic slip begin suddenly or do earthquakes begin slowly with accelerating fault slip? Do the size and duration of this precursory slip episode, if it occurs, scale with the magnitude of the eventual earthquake? Are there other precursors to an impending earthquake, such as changes in pore pressure, fluid flow, crustal strain, or electromagnetic field?

How do earthquake ruptures propagate? Do earthquake ruptures propagate as a uniformly expanding crack or as a 'slip pulse'? What is the effective (dynamic) stress during seismic faulting? How important are processes such as shear heating, transient increases in fluid pressure, and fault-normal opening modes in lowering the dynamic frictional resistance to rupture propagation?

How do earthquake source parameters scale with magnitude and depth? What is the minimum size earthquake that occurs on faults? How is long-term energy release rate partitioned between creep dissipation, seismic radiation, dynamic frictional resistance, and grain size reduction (i.e., by integrating fault-zone monitoring with laboratory observations on core)?

What are the physical properties of fault-zone materials and country rock (seismic velocities, electrical resistivity, density, porosity)? How do physical properties from core samples and downhole measurements compare with properties inferred from surface geophysical observations? What are the dilational, thermoelastic, and fluid-transport properties of fault and country rocks and how might they interact to promote either slip stabilization or transient overpressurization during faulting?

What processes control the localization of slip and strain? Are fault surfaces defined by background microearthquakes and creep the same? Would active slip surfaces be recognizable through core analysis and downhole measurements in the absence of seismicity and/or creep?

4.22.2 Fluids and Faulting

Among the many compelling reasons for drilling into active faults is the possibility to study the role of fluids, fluid pressure, and fluid flow in earthquake processes. A long-standing (and still-growing) body of evidence suggests that fluids are intimately linked to a variety of faulting processes (see review by Hickman *et al.* (1995)). These include the long-term structural and compositional evolution of fault zones; fault creep; and the nucleation, propagation, arrest, and recurrence of earthquake ruptures.

The concept that high fluid pressures and the localization of deformation are often linked is widely accepted in the structural geology literature (e.g., Hubbert and Rubey, 1959; Fyfe *et al.*, 1978), and has been reinforced by studies of active accretionary prisms in subduction complexes and their fossil equivalents (e.g., Dahlen, 1990; Fisher, 1996; Saffer and Bekins, 2006). Better understanding of the role of fluids in faulting in accretionary prisms is one goal behind the plan to drill in the Nankai subduction zone (the NanTroSeize project), as discussed below. A point to note is that there is good evidence that seismic rupturing, in at least some instances (e.g., the Western Taiwan fold and thrust belt and the western margin of the Great Valley adjacent to the San Andreas Fault), is occurring in fluid-overpressured crust (Davis *et al.*, 1983; Sibson, 1990). The Taiwan Chelungpu Fault Drilling Project (TCDP), discussed below, is related to drilling into the fault responsible for the *M* 7.7 Chi–Chi earthquake of 1999, which occurred along the western margins of the Western Taiwan fold and thrust belt.

4.22.2.1 Sources of Fault-Zone Fluids

Potential sources of fluids in brittle faults and shear zones include metamorphic fluid generated by dehydration of minerals during prograde metamorphism (including shear heating), fluid trapped in pore space as sedimentary formation brines, meteoric water carried downward by circulation, and release of volatiles from molten magma or the upper mantle (e.g., Kerrich *et al.*, 1984; Hacker *et al.*, 1995; Wakita and Sano, 1987; Ko *et al.*, 1997). The high fluid pressures that have been postulated within the San Andreas Fault Zone (being tested as part of the San Andreas Fault Observatory at Depth (SAFOD) drilling project discussed below) might be generated and maintained by continued upwelling of overpressured fluids within the fault zone and leakage of these fluids into the country rock (Rice, 1992). Alternatively, high fluid pressures might result from the sealing of locally derived high-pressure fluids within the fault zone once pressure gradients drop below a critical 'threshold' required to overcome forces between molecular water and mineral surfaces in very small cracks and pores (Byerlee, 1990).

Kennedy *et al.* (1997) argued that elevated $^3He/^4He$ ratios they observed in springs and wells located along a broad zone encompassing the San Andreas Fault system indicate that significant quantities of mantle-derived fluids are entering the fault zone through the ductile lower crust at near lithostatic pressure. However, without direct sampling of fluids from within the San Andreas Fault Zone at depth it is unclear whether these fluids are ascending through a broad, fractured, and faulted zone associated with the overall plate boundary or are narrowly focused within the (permeable) core of the San Andreas Fault itself, and hence intimately involved in the physics of faulting as envisioned by Rice (1992) and others.

4.22.2.2 Fault-Zone Permeability

The permeability structure of shear zones and brittle faults has recently been the focus of field studies that both confirm and extend observations made years ago by mining geologists. Large faults are not discrete surfaces but rather are a braided array of slip surfaces encased in a highly fractured and often hydrothermally altered transition or 'damage' zone (Smith *et al.*, 1990; Bruhn *et al.*, 1990, 1994; Chester *et al.*, 1993; Schulz and Evans, 2000). Structural and mineralogical textures indicate that episodic fracturing and brecciation are followed by cementation and crack healing, leading to cycles of permeability enhancement and reduction accompanied by episodic fluid flow along faults (e.g., Eichhubl and Boles, 2000).

Theoretical modeling (Sleep and Blanpied, 1992, 1994; Sleep, 1995) showed that the generation of dilatant pores and microcracks during earthquakes in a hydraulically isolated fault zone, followed by creep compaction between earthquakes, might lead to cyclically high fluid pressures along faults. Miller (1996) and Fitzenz and Miller (2003) have used the Sleep and Blanpied (1992) model to numerically simulate temporal variations in fluid pressure within faults and their role in controlling earthquake interactions and periodicity, making assumptions about the rheological and hydrological properties of fault and country rocks. However, using these models to predict the behavior of real faults in the Earth will require direct *in situ* measurements and sampling in active fault zones at seismogenic depths.

A possibly relevant development from studies of fluid pressure in sedimentary basins has been the revelation from borehole measurements of abrupt transitions, both vertically and laterally, between distinct fluid pressure regimes in some sedimentary basins. These 'fluid pressure compartments' are bounded by seals which in some cases are stratigraphic (e.g., shale horizons) but in others are gouge-rich faults or thin zones of hydrothermal cementation which cut across stratigraphy (Hunt, 1990; Powley, 1990; Dewers and Ortoleva, 1994; Martinsen, 1997). By analogy with these observations, Byerlee (1993) proposed a model in which contiguous vertical and horizontal seals within a fault zone would lead to discrete fluid pressure compartments (i.e., tabular lenses), the rupture of which might be important in earthquake nucleation and propagation (see Lockner and Byerlee (1995)). Although direct evidence for these fault-zone fluid compartments in active fault zones is lacking, negative polarity reflections (bright spots) on seismic reflection images acquired over some accretionary prisms have been interpreted to indicate the existence of high-pressure fluid compartments along the basal decollements (Moore and Vrolijk, 1992; Shipley *et al.*, 1994; Moore *et al.*, 1995; Bangs *et al.*, 2004).

4.22.2.3 Transient Fluid Pressure Effects

A range of physical effects arising from the mechanical response of fluid-saturated crust has been invoked to account for time-dependent phenomena associated with faulting such as slow earthquakes, creep events, earthquake swarms, and aftershock activity and its decay (e.g., Nur and Booker, 1972; Rice and Cleary, 1976; Dreger *et al.*, 2000; Hainzl and Ogata, 2005). Transient changes in fluid pressure and effective stress have also been suggested to play a direct role in rupture propagation and arrest. Shear resistance on the rupture surface may be dramatically lowered by localized increases in fluid pressure from frictional heating or locally elevated as a consequence of pore fluid diffusion and dilatant hardening at fault jogs and other irregularities (Sibson, 1973, 1985; Lachenbruch, 1980; Mase and Smith, 1987; Rudnicki, 1988; Sleep, 1995; Segall and Rice, 1995; Andrews, 2002). Continuous monitoring of fluid pressure within active, seismogenic faults are critical objectives of both the SAFOD and Gulf of Corinth scientific drilling project discussed below.

4.22.2.4 Chemical Effects of Fluids on Fault-Zone Rheology

Over the past several years a number of fault mechanics models have either been developed or refined that incorporate solution transport deformation mechanisms that may weaken and/or destabilize the fault zone. However, complicating this issue enormously is the fact that under only slightly varied environmental and mineralogical conditions similar processes can act to cement the fault zone together, thereby increasing fault strength (see Hickman and Evans (1992)). The experimental and theoretical studies on which these models are based are now focusing on processes that have long been inferred as being important from field observations of natural fault and shear zones, such as pressure solution, fluid-assisted retrograde mineral reactions, crack healing and cementation (e.g., Kerrich *et al.*, 1984; Power and Tullis, 1989; Bruhn *et al.*, 1990; Boullier and Robert, 1992; Chester *et al.*, 1993; Eichhubl and Boles, 2000). These deformation mechanisms are all interrelated, in that they depend upon thermally activated chemical reactions between the rock and pore fluid as well as the rates at which dissolved species are transported through the pore fluid.

Laboratory and theoretical investigations have shown that pressure solution may be important in reducing long-term fault strength and in promoting aseismic slip (i.e., creep) along faults (e.g., Rutter and Mainprice, 1979; Chester and Higgs, 1992; Bos and Spiers, 2001). In contrast, solution transport processes such as crack healing and sealing and cementation may cause the welding together of asperities or fault gouge, leading to time-dependent fault strengthening between earthquakes (e.g., Angevine *et al.*, 1982; Hickman and Evans, 1992; Karner *et al.*, 1997). Laboratory friction experiments conducted under hydrothermal conditions suggest that a change in dominant deformation mechanism with increasing depth from brittle deformation to solution transport creep might control the depth at which the seismic-to-aseismic transition occurs in the crust (Blanpied *et al.*, 1991). Observations of aligned fibrous serpentine in an exhumed branch of the San Andreas Fault system suggest that dissolution–diffusion–crystalization processes may be important in reducing fault strength and promoting aseismic slip (creep) along faults (Andreani *et al.*, 2005).

Hydrothermal mineral reactions can also weaken crustal rocks when the reaction products are weaker than the reactants (see Wintsch *et al.*, 1995). Based upon observations of exhumed shear zones in granite, Janecke and Evans (1988) argued that muscovite formed from the breakdown of feldspar might dramatically lower the ductile shear strength of the granite, even at temperatures well below those necessary for the plastic flow of quartz. At least at shallow depths, fault zones such as the San Andreas are mostly composed of clay- and mica-rich gouge resulting from the hydrolysis of feldspar (e.g., Wu, 1978), suggesting an enhancement of the feldspar breakdown reaction within the fault zone. Reactions in the olivine–talc–serpentine–water system have been demonstrated to dramatically lower the shear strength of ultramafic rocks in laboratory friction experiments (Pinkston *et al.*, 1987)

4.22.3 Frictional Strength of Faults

In addition to studying the role of fluids in faulting, fault-zone drilling provides the opportunity to directly measure the state of stress acting within and adjacent to active faults. As reviewed by Zoback and Healy (1984), Hickman (1991), and Townend and Zoback (2000), *in situ* stress measurements in a variety of faulting regimes, in conjunction with information on the attitude of nearby active faults, indicate fault strengths in intraplate areas that are comparable to those predicted by combining Coulomb faulting theory and laboratory derived coefficients of friction between 0.6 and 1.0 (Byerlee, 1978). This is sometimes known as Byerlee's law (Brace and Kohlstedt, 1980). When pore pressure is near hydrostatic (as has found to be the case at all sites where deep drilling has occurred in crystalline rock (see review in Townend and Zoback (2000)), high stress magnitudes, sometimes referred to as 'hydrostatic' Byerlee's law, are predicted. The high stress at depth consistent with Byerlee's law have been measured at a number of sites, including the Rocky Mountain Arsenal, Denver (Healy *et al.*, 1968); Rangely, Colorado (Raleigh *et al.*, 1972; Zoback and Healy, 1984); the Nevada Test Site (Stock *et al.*, 1985); the Fenton Hill geothermal site, New Mexico (Barton *et al.*, 1988; Fehler, 1989); Moodus, Connecticut (Baumgärtner and Zoback, 1989; Mrotek *et al.*, 1988); Dixie Valley, Nevada (Hickman *et al.*, 1997); the Siljian deep borehole in Sweden (Lund and Zoback, 1999) and to $\sim$8 km depth in the KTB drilling project, Oberfalz, West Germany (Brudy *et al.*, 1997). Thus, Byerlee's law (Brace and Kohlstedt, 1980), which was established on the basis of simple faulting theory and laboratory friction experiments (Byerlee, 1978), appears valid for faults within plate interiors. Studies of lithospheric flexure in response to sediment, volcanic, and internal loads (e.g., McNutt, 1980; McNutt and Menard, 1982; Kirby, 1983) also indicate that differential stresses in much of the Earth's crust are high and can approach the magnitude of stress predicted by Byerlee's law. Hence, such sources of stress are capable of generating crustal stresses large enough to induce faulting.

Figure 1 (from Townend and Zoback (2000)) shows a compilation of stress measurements in relatively deep wells and boreholes in various parts of the world. As shown, the ratio of the maximum and minimum effective stresses corresponds to a crust in frictional failure equilibrium with a coefficient of friction ranging between 0.6 and 1.0. The rate at which stress increases with depth is based on the assumption that the ratio of maximum to minimum effective stress is limited by ratio of shear to normal stress on pre-existing faults well-oriented to slip in the current stress field (see Zoback and Healy (1984)). Pore pressure was observed to be essentially equal to hydrostatic pressure at all the sites where deep drilling into crystalline rocks in the crust has taken place. Because stress magnitudes increase with depth due to increasing overburden stress, mean effective stress (mean stress minus the pore pressure, P_f) at depth scales approximately with depth as shown in the figure and discussed by Townend and Zoback (2000).

There are two implications of the data shown in **Figure 1**. First, Byerlee's law, defined on the basis of hundreds of laboratory experiments, appears to be applicable to faults *in situ*. The consistency of *in situ* friction coefficients and those measured in the lab is a rather amazing result when one considers the huge difference between the size of samples used for friction experiments in the lab and the size of real faults *in situ*, the variability of roughness of the sliding surface, and variability in the rock types encountered in the field and studied in the lab. Second, everywhere that stress magnitudes have been measured at appreciable depth, they indicate that they are controlled by the frictional strength of pre-existing faults in the crust. In other words, the Earth's crust appears to be in a state of frictional failure equilibrium and the law that describes that state is simple Coulomb friction.

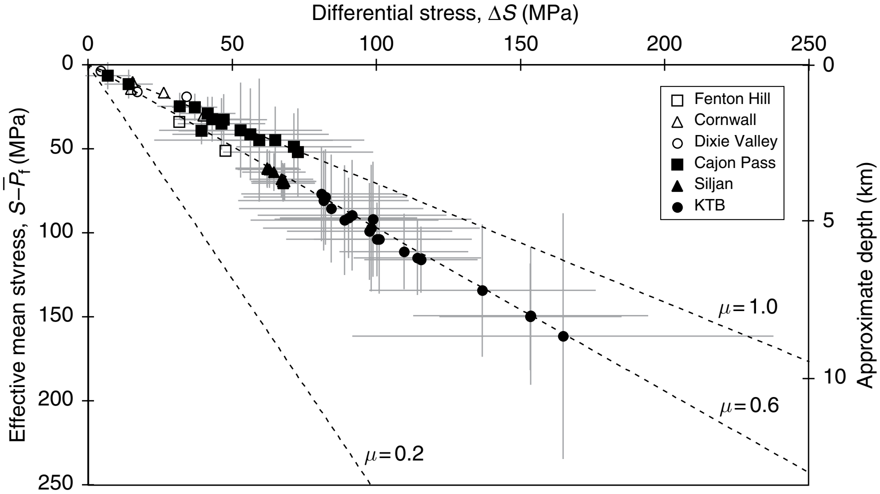

Figure 1 Stress measurements in deep boreholes indicate high crustal strength in accordance with Coulomb faulting theory with laboratory-determined coefficients of friction between 0.6 and 1.0 and hydrostatic pore pressure, which is observed in each borehole (after Townend and Zoback, 2000). It should be noted that the uncertainty estimates in the figure are likely significantly smaller than those shown.

4.22.3.1 Weak Plate-Bounding Faults

A substantial (and growing) body of evidence indicates that slip in crustal earthquakes along major plate-bounding faults (like the San Andreas) occurs at much low levels of shear stress than those shown in **Figure 1**. This hypothesis (sometimes referred to as the San Andreas Stress/Heat Flow Paradox, e.g., Lachenbruch and Sass, 1980, 1992; Zoback *et al.*, 1987; see review by Hickman (1991)). In the context of the San Andreas, there are two principal lines of evidence that indicate that the fault has low frictional strength – the absence of frictionally generated heat and the orientation of the maximum principal stress in the crust adjacent to the fault. A large number of heat flow measurements show no evidence of frictionally generated heat adjacent to the San Andreas Fault (Brune *et al.*, 1969; Brune, 1970; Henyey and Wasserburg, 1971; Lachenbruch and Sass, 1980, 1992; Williams *et al.*, 2004), which implies that shear motion along the fault is resisted by shear stresses approximately a factor of 5 less than those shown in **Figure 1**. Saffer *et al.* (2003) show that it is highly unlikely that topographically driven fluid flow has an appreciable effect on these heat flow measurements, indicating that the lack of frictionally generated heat in the vicinity of the San Andreas Fault is indeed indicative of average shear stress levels acting on the fault at depth.

In addition to the heat flow data, the orientation of principal stresses in the vicinity of the fault also indicates that right-lateral strike slip motion on the fault occurs in response to low levels of shear stress (Zoback *et al.*, 1987; Mount and Suppe, 1987; Oppenheimer *et al.*, 1988; Zoback and Beroza, 1993; Townend and Zoback, 2001, 2004). **Figure 2** (from Townend and Zoback (2004)) shows the direction of relative motion of the Pacific plate with respect to the North American plate indicated by GPS measurements with blue arrows (the map projection is about the pole of relative motion) and the direction of maximum horizontal stress (black, inward pointed arrows). The direction of maximum horizontal compression is clearly at a very high angle to the fault, resulting in low levels of resolved shear stress on the fault.

The significance of regional stress orientation for the state of stress on the fault at depth has been challenged by Scholz (2000) who argues that if stress orientations near the fault rotate to being ~45° from the strike of the fault, both the fault and the crust could have comparably high frictional strength. As summarized by Zoback (2000), there is appreciable evidence that even close to the fault the direction of maximum horizontal compression is at a high angle to the fault (Oppenheimer *et al.*, 1988; Zoback and Beroza, 1993; Townend and Zoback, 2001, 2004). In fact, stress measurements in the SAFOD pilot hole (Hickman and Zoback, 2004) located only 1.8 km from the San Andreas Fault in central California (discussed below) provide still more evidence in

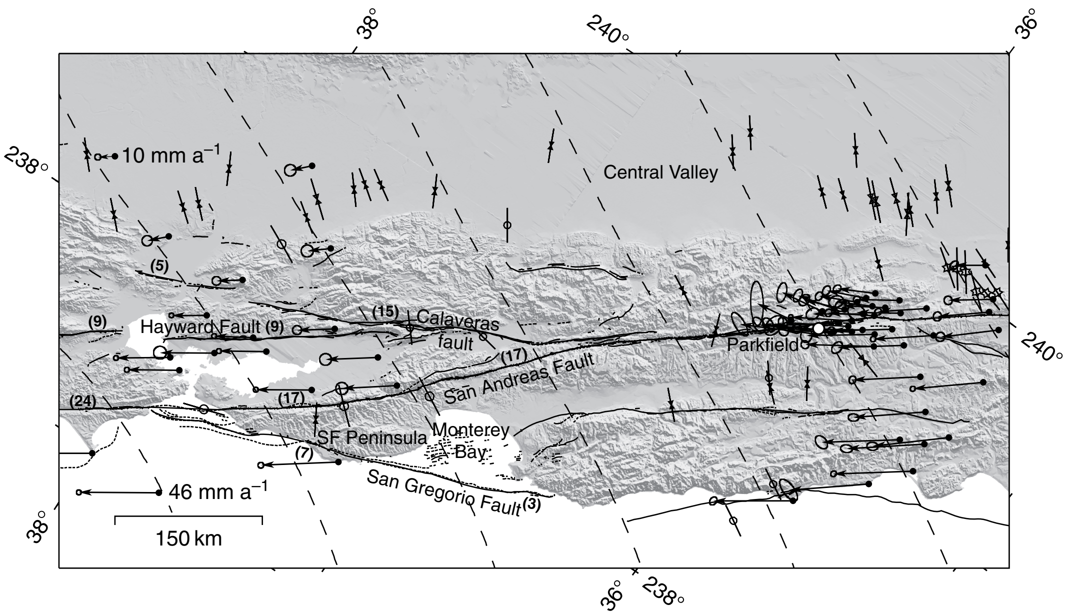

Figure 2 Maximum horizontal compressive stress (S_{Hmax}) and crustal velocity data from central California shown in an oblique Mercator projection about the North America–Pacific Euler pole. S_{Hmax} directions determined from borehole breakouts are shown by inward-pointing arrows, from hydraulic fracturing experiments by short line segments with stars, and from earthquake focal mechanism inversions by short line segments with split circles. The dashed trajectories show regional S_{Hmax} directions calculated using a model of lithospheric buoyancy and plate interaction by Flesch *et al.* (2000). The vectors illustrate crustal velocity data relative to North America (from Murray and Segall, 2001). The numbers in parentheses are Quaternary fault slip rates. The location of the SAFOD drillhole is shown by the open circle near Parkfield. After Townend J and Zoback MD (2004) Regional tectonic stress near the San Andreas fault in Central and Northern California. *Geophysical Research Letters* 31(13): L15S11.

support of the hypothesis that the San Andreas is a weak fault imbedded in a strong crust. In other words, stress magnitudes in the crust adjacent to the fault are high but shear stresses resolved on the fault are low.

Horizontal differential stress magnitudes in the pilot hole were found to be high adjacent to the fault (i.e., consistent with measurements shown in **Figure 1**) while the orientation of maximum horizontal stress at depth in the hole indicates low levels of shear stress resolved onto the San Andreas Fault itself (Hickman and Zoback, 2004). Shear-wave anisotropy measurements in the SAFOD main hole further indicate that the direction of maximum horizontal compression remains nearly perpendicular to the fault to within a few hundred meters of the active fault trace at depth (Boness and Zoback, 2006). In addition, heat flow measurements (to 2 km depth) in the SAFOD pilot hole are consistent with shallower data in the region which show no evidence of frictionally generated heat (Williams *et al.*, 2004).

There is mounting evidence that a number of other plate-boundary faults are similarly weak (see Lachenbruch and Thompson (1972), Kanamori (1980), Wilcock *et al.* (1990), Mount and Suppe (1992), Ben-Avraham and Zoback (1992), Magee and Zoback (1993), and Wang *et al.* (1995), and review by Hickman (1991). The concept that plate-bounding faults like the San Andreas are weak faults imbedded in a strong crust has become widely accepted in recent years and earthquake researchers are now faced with the problem of explaining why major plate boundary faults are substantially weaker than the surrounding crust. In fact, the question of how crustal faults lose their strength is critically important in crustal mechanics and earthquake hazard reduction for a number of reasons:

- As the weakness of plate boundaries (relative to plate interiors) is a fundamental aspect of plate tectonics, how and why plate boundary faults lose their strength is of fundamental global importance for understanding where plate boundaries form, how they evolve with time, and how deformation is partitioned along them.
- The roles of fluid pressure, intrinsic rock friction, chemical reactions, and the physical state of

active fault zones in controlling fault strength must be known in order to simulate earthquakes in the laboratory and on the computer using representative fault-zone properties and physical conditions. This information will also allow for improved models of static stress transfer and earthquake triggering at a regional scale and between specific faults, as needed for intermediate-term seismic hazard forecasting following large earthquakes.

- Through long-term fault-zone monitoring and *in situ* observations of the earthquake source, it will be possible to improve models for earthquake rupture dynamics, including such effects as transient changes in fluid pressure, fault normal opening modes and variations in slip pulse duration. These observations can be used directly in attempts to generate improved predictions of near-field strong ground motion (amplitude, frequency content, and temporal characteristics) and more reliable models for dynamic stress transfer and rupture propagation. The latter processes are believed to control earthquake size (i.e., whether or not a small earthquake will grow into a large one) and, hence, are crucial to long-term probabilistic assessments of earthquake hazard.
- The results of fault-zone drilling experiments are critical to the development of more realistic models for the seismic cycle and assessment of the practicality of short-term earthquake prediction in two ways. During fault-zone monitoring it will be possible to determine if earthquakes are preceded by accelerating fault slip (e.g., a nucleation phase) and/or transient changes in fluid pressure. Second, we will be able to determine whether or not factors which might dramatically lower fault strength (high pore pressure and/or chemical fluid–rock interactions, for example) are closely related to the processes controlling earthquake nucleation. Our current knowledge of fault-zone processes is so poor that not only are we unable to make reliable short-term earthquake predictions, we cannot scientifically assess whether or not such predictions are even possible.

In summary, while essentially all available data indicates that the frictional strength of intraplate crust is high, the frictional strength of plate-bounding faults is anomalously low. Taken together, the heat-flow data and the directional constraint (i.e., S_{Hmax} at 65–85° to the San Andreas Fault) suggest that the San Andreas Fault is weak in both an absolute and relative sense. In other words, the average shear stress required to cause faulting is low (comparable to earthquake stress drops), whereas the frictional strength of faults in the adjacent crust is much higher, consistent with Byerlee's law. Despite the fundamental nature of this finding, we have no direct *in situ* evidence indicating why this might be so, whether the mechanisms responsible for low strength along the San Andreas are likely to be found in other major fault systems or what role that these mechanisms might play in the processes of earthquake nucleation and propagation.

Numerous theories have been proposed over the past decade that are related to the weakness of the San Andreas and other plate-bounding faults. Knowledge of the *in situ* frictional properties of the San Andreas and other major active faults is not only of considerable scientific interest but is also critical for assessing the nature and potential magnitude of static stress transfer and earthquake triggering following large-to-intermediate size earthquakes.

Although the causes for the weakness of these faults are unknown, four general classes of explanations have been suggested:

- elevated fluid pressure (as discussed above);
- intrinsically low coefficients of friction of fault-zone materials;
- solution–transport reactions and related low stress deformation mechanisms (also discussed above); and
- dynamic weakening mechanisms such as shear heating/thermal pressurization or acoustic fluidization.

If the coefficient of friction, μ, is equal to 0.6–0.9 on the San Andreas Fault, as predicted by Byerlee's law, then the heat-flow constraint could be satisfied if the *in situ* pore pressure, P_p, is greater than twice hydrostatic (Lachenbruch and Sass, 1980, 1992). However, if one assumes that principal stress magnitudes are constant across the fault zone and that $\mu \geq 0.6$, then high fluid pressures alone cannot explain the directional constraint as P_p would exceed the least principal stress once the angle between S_{Hmax} and the fault exceeds about 60° (e.g., Zoback *et al.*, 1987; Scholz, 1989; Lachenbruch and McGarr, 1990). It has been suggested that large-scale yielding could lead to an increase in the magnitudes of the principal stresses within the fault zone relative to their values immediately outside of the fault (Rice, 1992). If so, this would allow P_p within the fault zone to exceed significantly the external magnitude of the least principal stress (Byerlee, 1990; Rice, 1992). In this manner, permanently high pore pressures within an intrinsically strong (i.e., high coefficient of friction) San Andreas Fault Zone, in conjunction with much lower fluid pressures in the surrounding rock, could lower the fault strength sufficiently to satisfy both the heat-flow and directional constraints.

A model that is, in many respects, similar to that of Rice (1992) was proposed earlier by Byrne and Fisher (1990) to explain the apparent weakness of the basal décollement beneath the Kodiak accretionary prism in southwest Alaska. Magee and Zoback (1993) applied the Rice model to explain the low frictional strength of the subduction zone associated with the $M \sim 8.2$ Tokachi-oki earthquake off northern Honshu, Japan. Although not requiring localized increases in stress magnitude, Fournier (1996) has presented a model in which near-lithostatic fluid pressures may be maintained within the San Andreas Fault Zone at depths greater than about 6–10 km if the maximum differential stress at these depths is quite low ($\sim$10–30 MPa) and the tensile strength of the rock outside the fault zone remains high due to pervasive crack healing at elevated temperatures.

Alternatively, if one assumes that the fault is optimally oriented with respect to the principal stresses and that fluid pressures are hydrostatic, then the heat-flow constraint can be satisfied if the friction coefficient along the fault is less than about 0.2 (Lachenbruch and Sass, 1992). Similarly, at least in central California where S_{Hmax} is at about 75–85° to the San Andreas Fault, the heat-flow and directional constraints can be simultaneously satisfied under conditions of uniformly hydrostatic fluid pressures if the friction coefficient is extremely low – about 0.1 or less – along the fault and Byerlee's law is applicable outside the fault zone (Lachenbruch and McGarr, 1990; Lachenbruch and Sass, 1992). It is often proposed that the presence of clays or other weak minerals along the San Andreas and other faults might lead to anomalously low frictional resistance (e.g., Wu 1978; Janecke and Evans, 1988; Wintsch *et al.*, 1995). This inference has been supported by laboratory sliding experiments on synthetic clay-rich fault gouges (e.g., Wang *et al.*, 1980; Shimamoto and Logan, 1981; Bird, 1984; Logan and Rauenzahn, 1987), on synthetic serpentinite gouges (Reinen *et al.*, 1994; Reinen and Tullis, 1995) and on synthetic laumontite gouge (Hacker *et al.*, 1995). However, these experiments are all at low-to-moderate confining pressures and temperatures. In contrast, experiments on natural clay-rich fault gouges collected from the San Andreas at depths of less than 0.4 km (Morrow *et al.*, 1982), on synthetic clay-rich fault gouges (Morrow *et al.*, 1992) and on synthetic serpentinite gouges (Moore *et al.*, 1997) at high temperatures and/or confining pressures and hydrostatic fluid pressures indicate coefficients of friction at *in situ* conditions that are too high to be reconciled with either the heat-flow or directional constraints. In addition, both natural and synthetic fault gouges deformed in the laboratory generally fail to exhibit the slip-weakening or velocity-weakening behavior required for the generation of earthquakes (e.g., Byerlee and Summers, 1976; Logan and Rauenzahn, 1987; Marone *et al.*, 1990; Morrow *et al.*, 1992; Reinen *et al.*, 1994). Thus, the importance of these materials in the rheology of the San Andreas Fault at seismogenic depths is unclear.

Another important class of models that might explain the low long-term strength of seismically active segments of the San Andreas and other major faults have called upon processes directly associated with earthquake rupture propagation. These dynamic weakening mechanisms include shear heating during slip, leading to transient high fluid pressures (Lachenbruch, 1980; Andrews, 2002) or melting (Sibson 1973; Spray, 1987; Rice, 2006); reductions in normal stress accompanying the propagation of dilational waves along the fault (Brune *et al.*, 1993; Andrews and Ben-Zion, 1997); the fluidization of fault-zone materials due to the channeling of co-seismic acoustic energy (Melosh, 1979, 1996); and hydrodynamic lubrication (Brodsky and Kanamori, 2001). While such processes may be operative during an earthquake, they do not relate to the problem of how earthquakes initiate and each requires that very specific fault-zone conditions exist to be viable. Thus, to assess the likelihood that dynamic weakening mechanisms might operate along active faults we need to compare the structure and physical properties of actual fault zones with parameters required by these various models and then combine these observations with the results of long-term fault-zone monitoring in the near field of small-to-moderate size earthquakes.

4.22.4 Near-Field Observations of Earthquake Nucleation and Propagation

Understanding the physical processes operating during both nucleation and rupture propagation can prove to be critical to understanding why plate boundary faults tend to be anomolously weak, especially if dynamic weakening mechanisms are important. In addition, by drilling into active faults at seismogenic depths and observing repeating earthquakes at very short distances, one can observe near-field phenomena for earthquakes of $M \sim 1$ or larger, thereby providing a new window into the physics of the earthquake source. Ideally, in addition to instrumenting fault-zone drill holes with seismometers, it would be ideal to place instruments within or immediately adjacent to active sliding surfaces to directly monitor fault displacement, deformation, pore pressure, and heat generated during sliding. The work of Brune and co-workers on foam rubber models of earthquakes (Brune *et al.*, 1993; Anooshehpoor and Brune, 1994) illustrates the advantages of making measurements at or very near the sliding surface. Many of the objectives for near-field observation would be met by sensors placed within a few hundred meters of the earthquake source. At these distances, near-field waves will be of significant amplitude compared to the far-field waves for $M \geq 0$ events, and static strains will be well within the resolution of borehole strainmeters.

The process by which the fault becomes unstable and initiates a dynamically propagating rupture is central to understanding how earthquakes work. It has recently been proposed that the very beginnings of rupture for earthquakes in the magnitude range from at least $M_w = 1$–8 characteristically involve a period of slow growth of the seismic moment (Iio, 1992, 1995; Ellsworth and Beroza, 1995, 1998; Beroza and Ellsworth, 1996). The characteristics of this process, called the seismic nucleation phase, rule out self-similar models for the nucleation and growth of rupture including the standard model of a dynamically growing crack (Kostrov, 1964). Although a range of hypotheses have been proposed to explain this slow beginning to earthquakes, far-field observations have thus far proved to be inadequate to determine if the seismic nucleation phase represents a cascade of smaller events, in which case the dynamically expanding crack model might apply, or if it represents a transition from an aseismic (stable) sliding to dynamic rupture, as required by laboratory-based and theoretical models of rupture initiation (Dieterich, 1992; Ohnaka, 1992). Observations of the nucleation process made within the near field in drill holes passing close to or through active faults at seismogenic depths have the potential to resolve this process, as they will not be distorted by attenuation or scattering, which limits the interpretation of available data (Iio, 1995).

The physics of earthquake rupture propagation has also been the subject of intensive investigation in recent years (e.g., Heaton, 1990; Brune *et al.*, 1993; Melosh, 1996; Peyrat *et al.*, 2004; Harris, 2004). New data have again drawn into question the standard model of a dynamically expanding crack that heals inward from its outer boundary (Madariaga, 1976). There is now evidence from large earthquakes that the rupture may propagate as a 'slip pulse' (e.g., Wald and Heaton, 1994), yet we know little about how such a concentrated slip zone is generated or maintained, or why the fault comes to rest so abruptly. Brune *et al.* (1993) have further proposed that tensile opening of the fault accompanies the shear displacement in the slip pulse. If correct, it would be a mechanism by which a fault can have high static strength, but slide without generating heat. However, sliding at near-zero normal stress implies that the dynamic stress drop should equal the tectonic stress (see Lachenbruch and Sass (1980)) resulting in near-zero shear stress on the fault after rupture (e.g., Zoback and Beroza (1993) for the Loma Prieta earthquake). Thus, measuring the dynamic stress drop in the near-field region will give us a direct test of the high static strength/low dynamic friction hypothesis.

Recent observations of microearthquakes in moderately deep boreholes (2–2.5 km) at Cajon Pass, California (Abercrombie and Leary, 1993; Abercrombie, 1995), the SAFOD pilot hole (Imanishi *et al.*, 2004), and in Long Valley, California (Prejean and Ellsworth, 2001) demonstrate that ultra-high-fidelity recordings can be made in downhole observatories. Imanishi and Ellsworth (in press) recently used high-frequency recordings from the SAFOD Pilot Hole array to study the scaling of apparent stress (seismic wave energy/seismic moment). They found that this ratio shares the same upper bound over the magnitude range from $M9$ to $M0$, providing strong support for the self-similar model of the earthquake source.

4.22.5 Fault-Zone Drilling Projects

In this section we review several recent, on-going, and planned scientific drilling projects related to earthquake studies. Many of the key questions to be addressed by deep drilling into active faults were enumerated in December 1992 at a workshop (attended by 113 scientists and engineers from seven countries) on San Andreas Fault-Zone drilling at the Asilomar Conference Center in Pacific Grove, California. While the purpose of this workshop was to initiate a broad-based scientific discussion of the issues that could be addressed by drilling and direct experimentation in the San Andreas Fault, the arguments put forth for scientific drilling into fault zones are generally applicable to all of the fault-zone drilling projects discussed in this section.

The questions to be addressed by fault-zone drilling projects are far reaching, and include the following:

4.22.5.1 Fault Behavior

- What is the static strength of active faults? Why are some faults anomalously weak?
- Why are some faults (or fault segments) creeping and some locked?
- What factors control the localization of slip and strain?
- How are faults stressed at different crustal levels?
- How does strain communication occur within fault zones over different time scales?
- How is energy partitioned within fault zones between seismic radiation, frictional dissipation, grain-size reduction, and chemical reactions?
- Can the frequency–magnitude relationship for earthquakes be extrapolated to smaller magnitudes?

4.22.5.2 Fluid Pressure

- What is the vertical and lateral distribution of fluid pressure regimes in faults?
- Do fault fluid pressure compartments exist?
- If so, what is the nature of the seals between these compartments?
- What is the time dependence of fluid pressure within fault zones?
- What is extent of vertical and lateral fluid migration during a seismic stress cycle?

4.22.5.3 Fault Fluids

- What is the origin and composition of fault zone fluids?
- What are the permeabilities of fault-zone materials and country rock?
- What are the fluid transport mechanisms in and adjacent to fault zones and what physical processes lead to fluid redistribution?
- What is the interplay between water–rock interaction and rheology at different structural levels?

4.22.5.4 Fault-Zone Properties and Physical Parameters

- How does the stress tensor vary in the vicinity of fault zones?
- How do pre- and postfailure stress states compare?
- What, if any, form of cyclical dilatancy operates in the vicinity of fault zones?
- How do physical properties relate to the fault zone fabric?
- What is the origin of low-velocity zones associated with fault zones?
- How well and in what manner do physical properties and heterogeneity measured in boreholes correlate with geophysical observables?

4.22.5.5 Fault Structure and Materials

- How does the width and character of active slip zones vary with depth?
- What is the thermal structure of active fault zones?
- How do mineralogy and deformation mechanisms within fault zones change with depth, temperature, and country-rock geology?
- What determines the maximum depth of seismic activity?
- At what temperature do mineral reaction kinetics operate at the timescale of an earthquake cycle?
- How accurate are inferences drawn from deformation microstructures, piezometers, and fluid inclusions and how might one assess their survivability?

Fundamental questions about faulting and earthquakes such as these have gone unanswered due to the complete lack of data on the physical and chemical processes operating on faults at depth. Hence, the principal reasons for drilling into active faults are to conduct extensive investigations *in situ* and on exhumed materials that are representative of the faults at the pressures, temperatures, and conditions at which major earthquakes nucleate.

4.22.5.6 San Andreas Fault Observatory at Depth

The site identified for this 3.0 km deep drilling project is located in central California (**Figure 2**), about 10 km northwest of the town of Parkfield. This site is located at the northwestern end of the rupture zone of the 1966 and 2004 $M = 6$ Parkfield earthquakes, in the transition between the creeping and locked sections of the San

Andreas Fault. The San Andreas displays a range of behaviors at this site. At the surface, the fault is creeping at a rate of 1.8 cm yr^{-1}, with most of the fault displacement localized to a zone no more than 10 m wide (Burford and Harsh, 1980; Schulz, 1989). Numerous earthquakes occur directly on the San Andreas Fault in the depth interval from about 3 to 12 km. The shallow seismicity at Parkfield occurs in tight clusters of activity (Nadeau *et al.*, 1994; 1995, 2004) that have remained spatially stationary for at least the past 20 years.

An important feature of the microearthquakes beneath Middle Mountain is that they occur in families of repeating events which provide a reliable target for guiding drilling (**Figure 3**). Individual earthquakes have been observed to recur numerous times using the U.C. Berkeley High Resolution Seismic Network (HRSN), at precisely the same location and with the same magnitude (Nadeau *et al.*, 1994, 1995, 2004; Nadeau and McEvilly, 1997). Repeating sources of up to $M = 2$ are located at drillable depths beneath the proposed drill site. A major goal of this experiment is to drill as close as possible to one or more of these sources and to follow the buildup of strain and its release through multiple earthquake cycles during the monitoring phase of the experiment.

Illustrated in **Figure 3**, a 2 km deep pilot hole drilled at the SAFOD site in 2002, 1.8 km to the southwest of the surface trace of the San Andreas Fault (see review by Hickman *et al.* (2004) and associated papers published in special issues of Geophysical Research Letters). During the summers of 2004 and 2005, the SAFOD mainhole was rotary drilled through the zone of the repeating microearthquakes. Note that in the subsurface, the position of the fault is to the southwest of the surface trace.

Four major geologic units were encountered along the trajectory of the SAFOD main hole: In the vertical section of the wellbore, the near-surface Quaternary and Tertiary sediments were found to be underlain by Salinian granite at a depth of ~700 m. After deviating the borehole toward the fault, arkosic sediments (most likely locally derived from Salinian granite) were encountered about 300 m NE of the drill-site, perhaps after crossing the Buzzard Canyon fault, a NW trending strike-slip fault exposed at the surface that trends subparallel to the San Andreas (M. Rymer, personal communications). Approximately, 1200 m NE of the drillsite, a possibly ancestral trace of the San Andreas was crossed as the lithology changed abruptly to claystones and siltstones of the Great Valley formation, found throughout central California on the east side of the San Andreas.

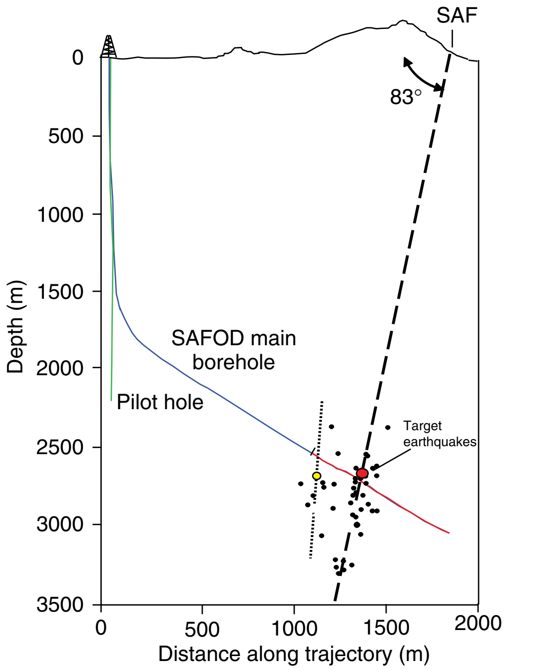

Figure 3 Schematic diagram of the SAFOD pilot hole and main hole. The precise location of the target earthquakes is approximate although the relative locations are exact. As indicated by the distribution of microearthquakes, slip is accommodated by multiple faults at depth. Simply connecting the position of the San Andreas Fault at depth with the surface position implies that the fault dips steeply to the west.

Geophysical logs and cuttings analysis indicate that the San Andreas is a broad zone of anomalously low P- and S-wave velocity and resistivity that define a relatively broad damage zone as indicated in **Figure 4**. The locations of active fault traces are revealed by casing deformation (indicated by the red line in **Figure 4**) and the location of a $M \sim 0$ microearthquake that occurred in May 2005 (indicated in **Figure 4**). Note that these active faults are associated with narrower, more highly localized zones of low P- and S-wave velocity and resistivity embedded within the broader damage zone. In a third phase of the project, coring will be done in multilateral holes to directly sample the damage zone and both creeping/seismically active faults at depth. Preliminary results from the project were presented in several special sessions of the December 2005 American Geophysical Union meeting (published in EOS, v. 86, 2005), and numerous publications are in print or under review detailing early results from SAFOD.

An array of downhole seismometers, accelerometers, and other sensors will be deployed near

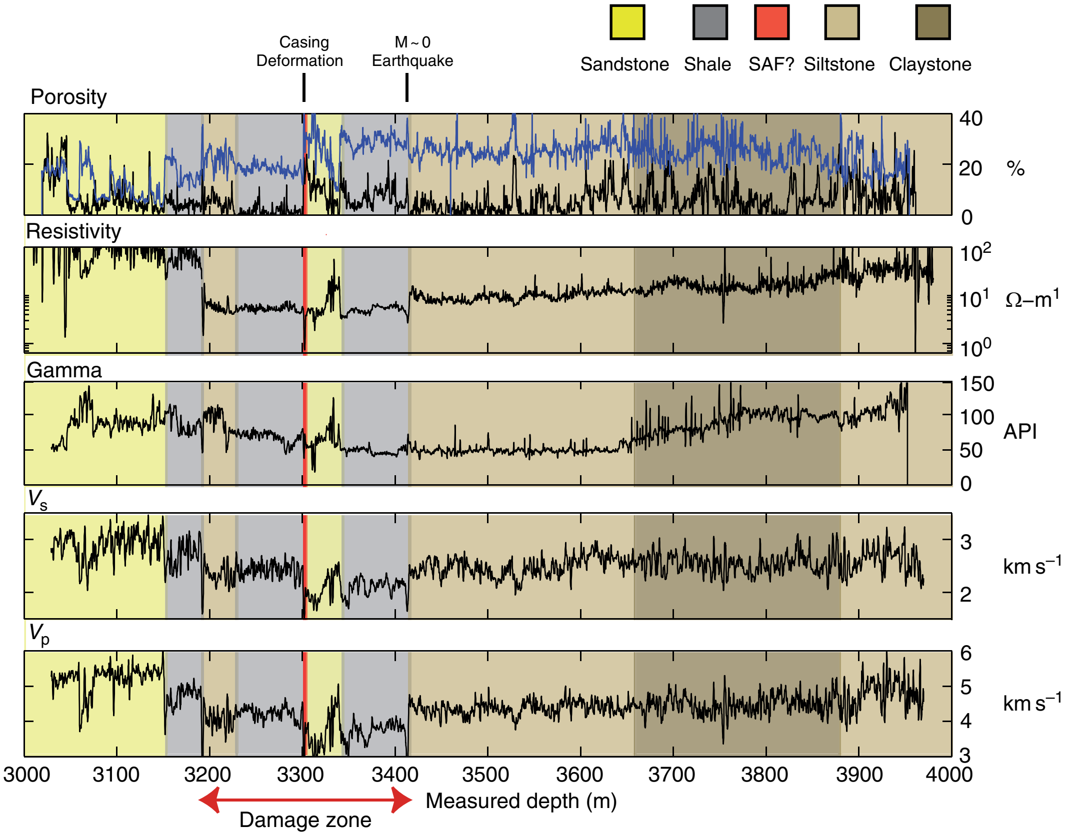

Figure 4 Geophysical logs and generalized lithology from phase 2 of the SAFOD project (shown in red in **Figure 3**). Anomalously low V_p, V_s, and resistivity indicate a broad low damage zone ~250 m wide. Multiple active fault traces appear to occur within the damage zone. The red line at 3300 m depth indicates an area of localized casing deformation. A $M \sim 0$ earthquake was recorded by a seismic array in the borehole appears to be associated with the localized low velocity zone at 3410 m.

the fault zone after drilling. This will allow for accurate determinations of the radiated energy, seismic moment, and earthquake locations can be made, the detailed velocity structure of the fault zone can be investigated, and earthquake nucleation and propagation can be studied with unprecedented detail. High-frequency signals are expected from the very local events, with good signal-to-noise above 1 kHz. Thus, good sensitivity to the higher frequencies becomes the most important seismic monitoring design criteria. Peak acceleration estimates for a magnitude 1.0 earthquake located at a distance of 1000 and 100 m are 1*g* and 10*g*, respectively.

4.22.5.7 Nojiima Fault

In 1995, a *M* 6.9 strike-slip faulting earthquake struck Kobe, Japan, resulting in 6432 fatalities. The earthquake occurred on the Nojiima Fault (**Figure 5**), a right-lateral strike-slip fault that trends NE–SW through Awaji Island and beneath Osaka bay (Ando, 2001). Several research groups drilled boreholes (ranging in depth from 747–1800 m) through the fault along segments of the Nojima Fault that exhibited surface rupture during the earthquake. Note the numerous shallow (2–5 km depth) occurred on the Nojiima Fault beneath Awaji Island. Extensive geophysical logging, detailed core analysis, stress measurements, and repeated hydrological tests and repeated injection tests were carried out. The preliminary results were published in the special volume of the Island Arc (Oshiman *et al.*, 2001).

Two boreholes were drilled at Hirabayashi (where the maximum slip was 2 m) that penetrated the core of the Nojima Fault. The structure of the Nojima Fault Zone is characterized by a narrow fault core with various types of fault gouge. The hanging wall of the fault displays many minor shear zones that increase in frequency toward the fault core (**Figure 6**). The footwall of the fault is significantly

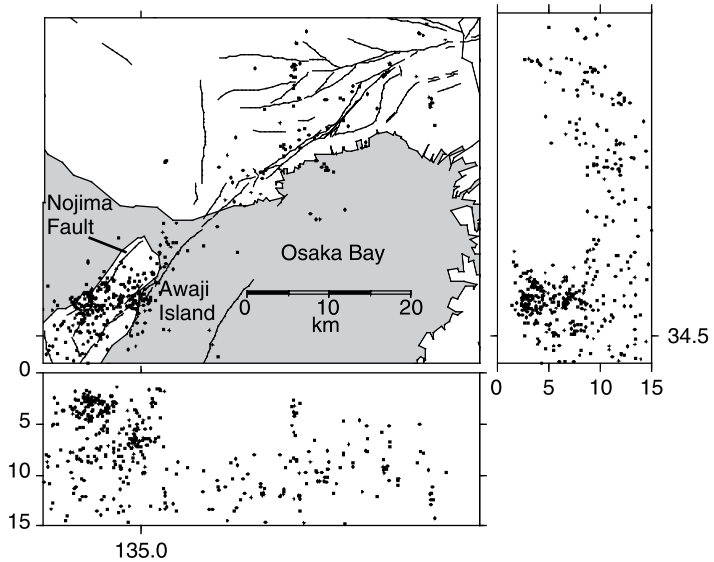

Figure 5 The Nojima Fault – source of the *M* 6.9 1995 Kobe earthquake – is an NE trending strike-slip fault exposed on Awaji Island and extends beneath Osaka Bay. Numerous shallow aftershocks (black dots) occurred on the section of the fault where drilling took place. East–west and north–south cross-sections show the distribution of aftershocks with depth. As shown, many of the aftershocks beneath Awaji Island are extremely shallow (2–5 km deep), with others extending to typical depths of 10–15 km. Courtesy of H. Ito.

less deformed and less altered with respect to the hanging wall. The physical properties of fault zone and country rocks have been extensively studied (Tanaka *et al.*, 2001; Ohtani *et al.*, 2001; Fujimoto *et al.*, 2001; Boullier *et al.*, 2001).

Integrated borehole monitoring systems (three-component strain meter, three-component seismometer, and water-level sensors) have been installed along two different segments of the Nojima Fault.

4.22.5.8 Chelungpu Fault

The 1999 *M* 7.7 Chi–Chi earthquake in Taiwan produced large zones of surface rupture, with a maximum displacement of 8 m on the Chelungpu Fault. Along nearly all of its length, the earthquake fault strikes ~N–S (**Figure 7(a)**) with the rocks to the east thrust over those to the west along an east-dipping thrust faults (**Figure 7(b)**). The northern portion of the fault is characterized by very large slip but relatively low ground acceleration during the *M* 7.7 earthquake. The Taiwan Chelungpu Fault Drilling Project (TCDP) was carried out near the town of Dakeng in a zone of large surface offset (and subsurface slip) near the northern end of the N–S trending rupture surface.

The main scientific objectives for drilling were related to testing various mechanisms of nucleation and rupture of large earthquakes and provide answers to fundamental questions pertaining to the relationship between the Chelungpu thrust and regional tectonics (Tanaka *et al.*, 2002; Ma *et al.*, 2003). TCDP drilling was started in 2004 and two boreholes were completed in 2005, including successful continuous coring, logging, and borehole monitoring. The direction of maximum horizontal compression found in one of the TCDP boreholes is ~N 120° E, consistent with the regional stress field (Kao and Angelier, 2001) and relative motion of the Phillipine Sea Plate with respect to Taiwan (Wu *et al.*, 2007).

As shown in **Figure 8**, two holes (A and B) were drilled through the main fault zone that ruptured during the Chi–Chi earthquake (**Figure 8**). In hole A, multiple fault zones were identified in the Pliocene Chinshui Shale and Miocene Kueichulin Formation, but the primary slip zone in hole A was encountered at a depth of 1111 m (see photo in **Figure 8**) and 1136 m in hole B (see photo in **Figure 8**). This fault is associated with bedding-parallel thrusting with a gentle dip of about 20° and is characterized by over 1 m thickness of gouge (fault core) and gradational breccia in a damage zone found in both the upper and lower blocks. Wu *et al.* (2007) noted a major perturbation of the stress field in hole A in the vicinity of the Chelungpu Fault.

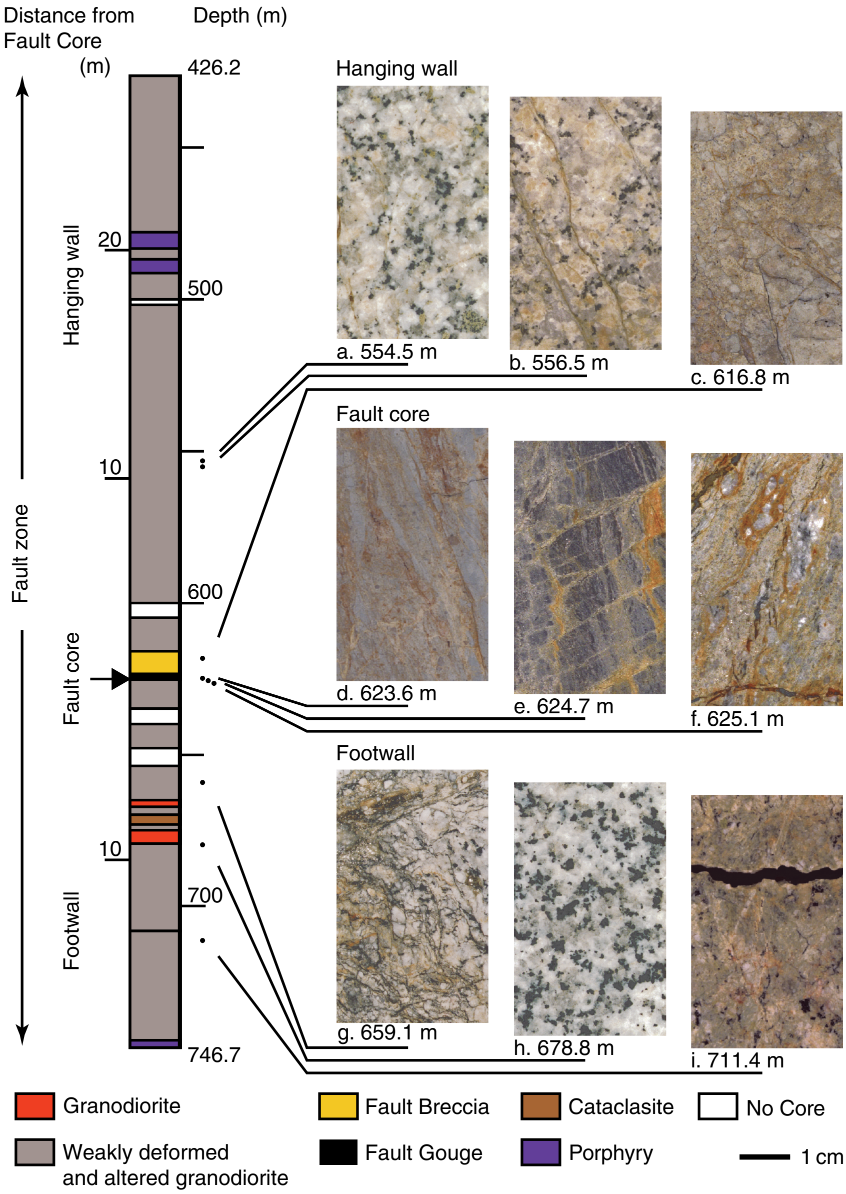

Figure 6 Lithologies encountered in the Nojima Fault and photographs of rocks from the hanging wall, fault core, and footwall. After Ando M (2001) Geological and geophysical studies of the Nojima Fault from drilling: An outline of the Nojima Fault Zone Probe. *The Island Arc* 10: 206–214.

To address key questions of earthquake rupture dynamics such as energy dissipation and fracture energy, Ma *et al.* (2006) analyzed the grain size distribution of the fault gouge. They estimated that 6% of the total earthquake energy is associated with gouge formation. Tanaka *et al.* (2007) and Kano *et al.* (2006) discuss the possibility that a thermal anomaly measured at the trace of the fault is associated with frictional heat generated during faulting.

4.22.5.9 Gulf of Corinth

The Gulf of Corinth, Greece, is the most actively deforming region in Europe and one of the most seismically active areas. Deformation in the area is dominated by north–south directed back-arc extension associated with the Hellenic trench. The Gulf of Corinth is an east–west trending graben bordered on the north and south by east–west trending normal faults (**Figure 9**). The extension rate in the region

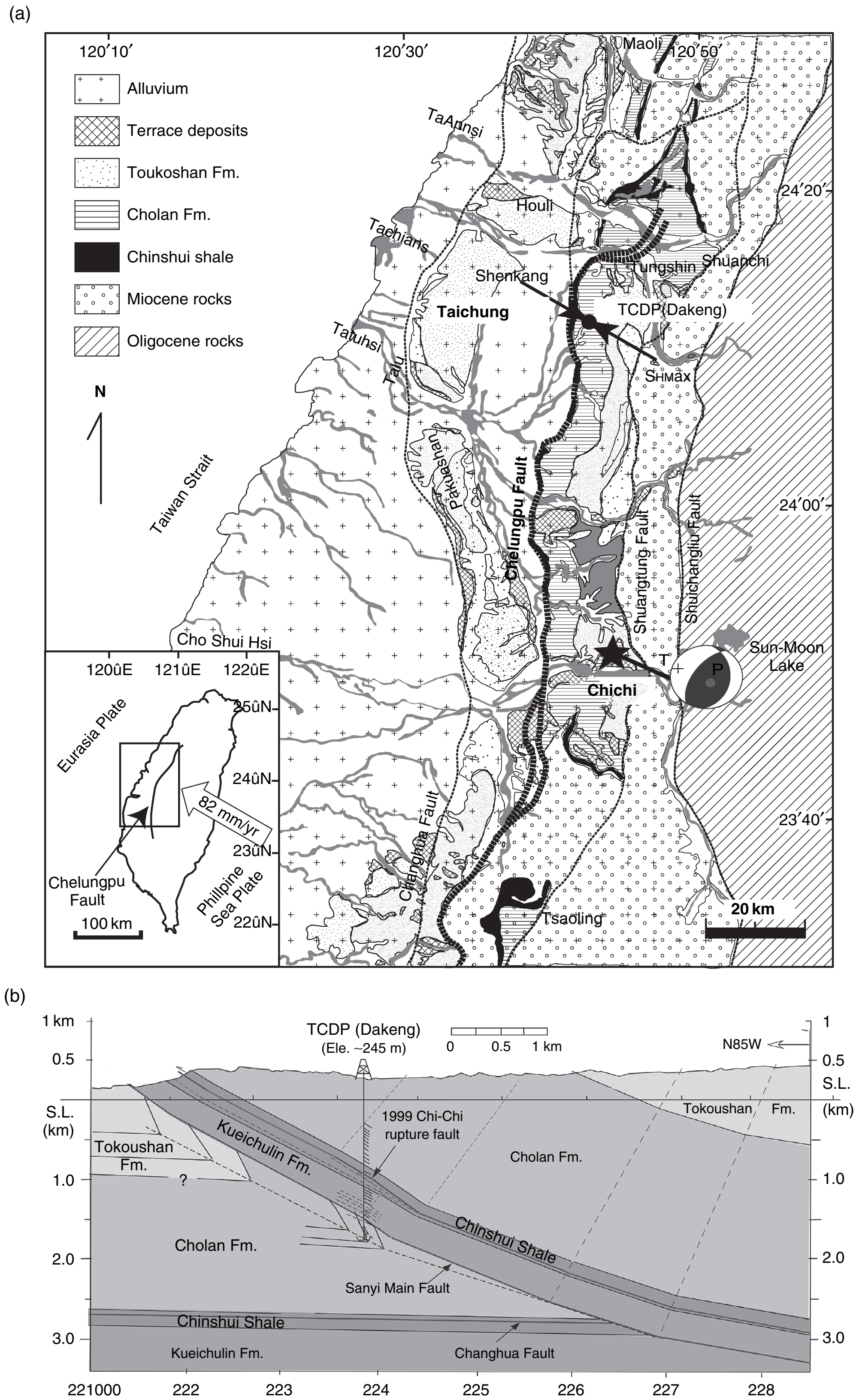
(a)
120′10′
120′30′
120′50′
24′20′
24′00′
23′40′
Alluvium
Terrace deposits
Toukoshan Fm.
Cholan Fm.
Chinshui shale
Miocene rocks
Oligocene rocks
N
Maoli
TaAnnsi
Houli
Tachians
Shenkang
Tungshin
Shuanchi
Taichung
TCDP (Dakeng)
Tatuhsi
Tatu
SHmax
Taiwan Strait
Pakuashan
Chelungpu Fault
Shuangtung Fault
Shuichangliu Fault
Cho Shui Hsi
Sun-Moon Lake
T
P
Chichi
Changhua Fault
Tsaoling
20 km
120ûE
121ûE
122ûE
25ûN
24ûN
23ûN
22ûN
Eurasia Plate
82 mm/yr
Chelungpu Fault
Phillpine Sea Plate
100 km
(b)
1 km
0.5
S.L.
(km)
1.0
2.0
3.0
TCDP (Dakeng)
(Ele. ~245 m)
0
0.5
1 km
N85W
1
0.5
S.L.
(km)
1.0
2.0
3.0
Tokoushan Fm.
Tokoushan Fm.
?
Kueichulin Fm.
1999 Chi-Chi rupture fault
Cholan Fm.
Cholan Fm.
Chinshui Shale
Sanyi Main Fault
Chinshui Shale
Kueichulin Fm.
Changhua Fault
221000
222
223
224
225
226
227
228

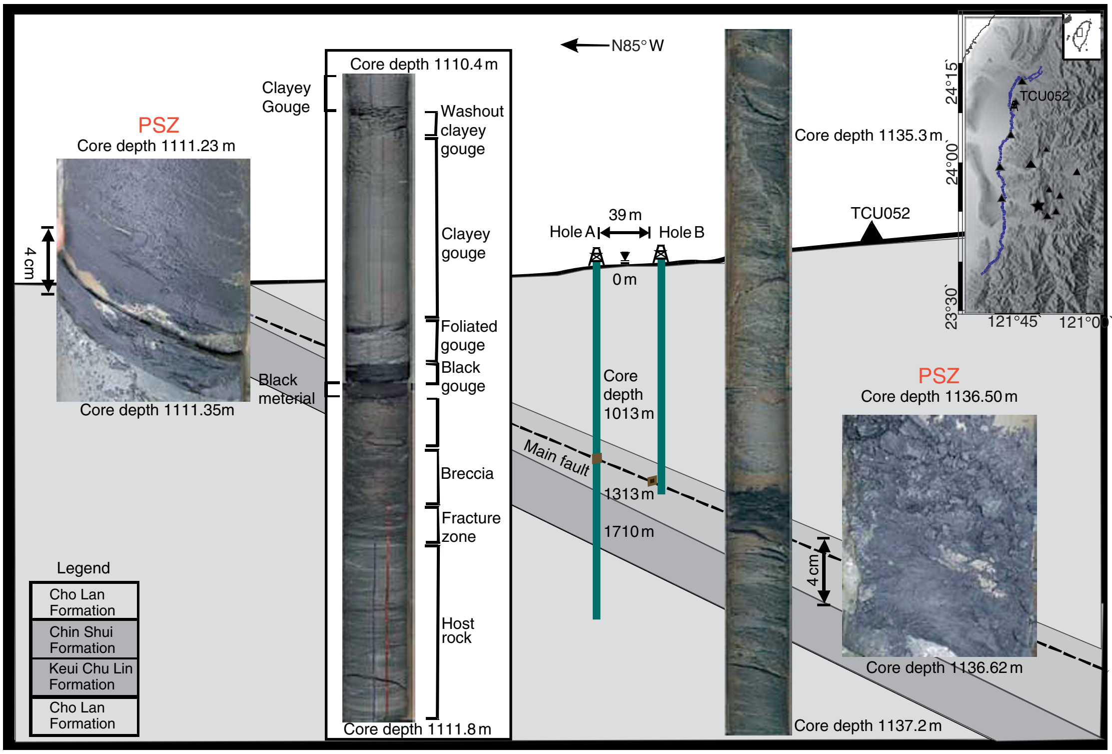

Figure 8 Detailed ithologies and fault rocks encountered in the two TCDP core holes shown on a background of the generalized geology as shown in **Figure 7(b)**. The primary slip zone in hole A was encountered at a depth of 1112.23–1111.35 m (see photo) and 1136.50–1136.62 m in hole B (see photo). Courtesy of K.-F. Ma.

ranges between 1 and 1.5 cm yr^{-1}. A number of large earthquakes have occurred in the region in the past century.

The Corinth Rift Laboratory (CRL) project involved drilling into the Aigion Fault on the south side of the Gulf. This site offers excellent conditions for *in situ* investigation of active normal faulting, the rifting process and for monitoring fluid–fault interactions (Cornet *et al.*, 2004).

The AIG10 borehole was drilled in 2002 to 1000 m depth and intersected the Aigion Fault at 760 m (**Figure 10**). A key goal of the laboratory is to understand the relationships between outcrops of steeply dipping fault zones and the seismogenic faults at great depth. Special attention is directed to the interactions between circulating fluids and fault mechanics, including hydro-thermo-mechanical coupling and the role of geochemical healing and alteration. After passing through an overburden of sands, conglomerates, and clays, the borehole penetrated alternating Mesozoic radiolarite and limestone in the hanging wall before intersecting the main fault zone at a depth of 760 m, where cataclastic fault rocks were encountered. Below the fault, a homogeneous, heavily karstified limestone was encountered down to 1000 m.

The Aigion Fault Zone forms a hydraulic barrier that sustains about a 0.5 MPa differential pressure across it. There is a slight overpressure (~0.5 MPa) in the hanging wall immediately above the fault with a larger overpressure (0.9 ± 0.1 MPa) in the foot-wall resulting from the topographic relief from the footwall to the hanging wall sides of the fault. Nearly

Figure 7 (a) Generalized map of surface geology in western Taiwan (H. Tanaka, personal communication, 2006), the trace of the Chelungpu Fault that slipped in the *M* 7.7, 1999 Chi–Chi earthquake epicenter and the location of the TCDP boreholes near Dakeng are shown. The average ~N120° E direction of maximum horizontal compression observed in the borehole (Wu *et al.*, 2007) is the same as the regional stress field (Kao and Angelier, 2001) and the motion direction of the Phillipine Sea Plate relative to Taiwan (see inset). (b) Geologic cross-section derived from high-resolution seismic reflection data showing the location of the TCDP borehole with respect to the east dipping Chelungpu Fault. After Yue LF, Suppe J and Hung JH (2005) Structural geology of a classic thrust belt earthquake: The 1999 Chi-Chi earthquake Taiwan (M 7.6). *Journal of Structural Geology* 27: 2058–2083.

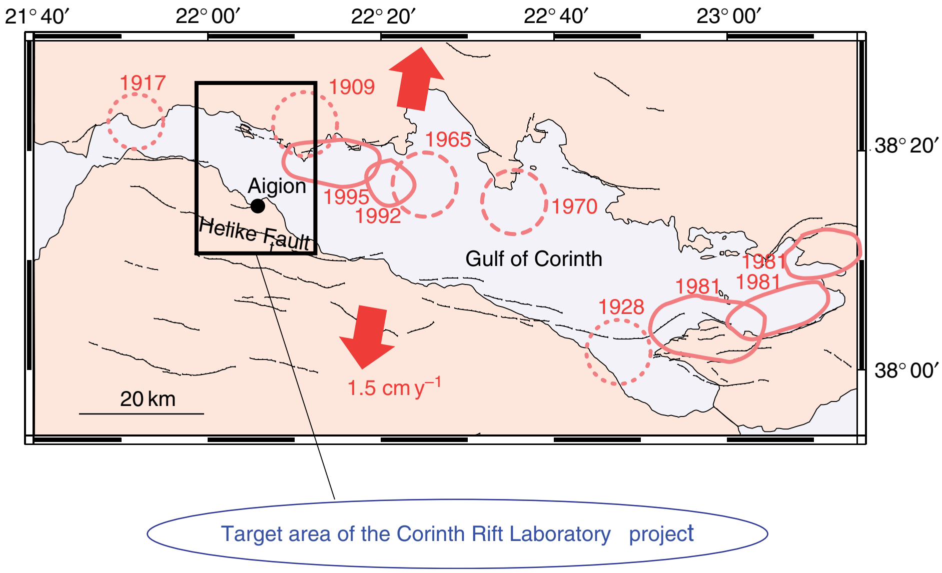

Figure 9 Active tectonics of the Gulf of Corinth area showing the locations of active normal faults, large earthquakes of the past 100 years, and geodetically determined extension directions and rates. Courtesy of F. Cornet.

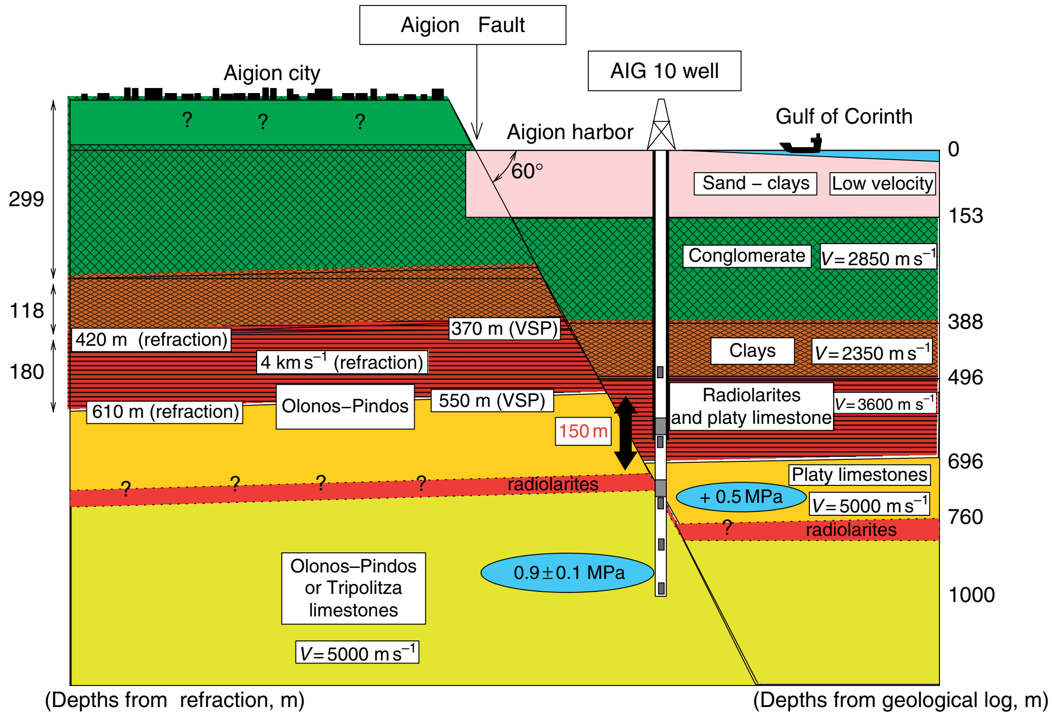

Figure 10 Geology in the vicinity of the AIG 10 well that was cored through the Aigion Fault. The fault was encountered at a depth of ~760 m. Pore pressure on the footwall side of the fault at depth was approximately 1 MPa in excess of hydrostatic, consistent with the fact that the footwall elevation is approximately 100 m higher than the elevation of the well. Courtesy of F. Cornet.

isothermal temperatures (31 °C) below the fault is consistent with local convection in the karstic limestone while an absence there is an absence of flow above the fault. Geochemical data indicate a shallow continental origin of water in and adjacent to the fault zone, with a notable absence of deep fluid input from the mantle. The borehole is being used to make continuous measurements of pressure in the fault zone.

The data acquired to data show tidal variations, as well as pressure variations induced by remote earthquakes (Cornet *et al.*, 2004). The Corinth science team proposes to drill a 4.5 km deep borehole to monitor transients in pore pressure within the seismogenic zone and provide clues to the origin of deep fluids.

4.22.5.10 NELSAM

The deep gold mines of South Africa offer unique environments to study earthquakes by providing access to the focal area. The mining operations generate thousands of earthquakes per day, and some of these events approach M 5. The Natural Earthquake Laboratory in South African Mines (NELSAM) is a project that utilizes the availability of these deep mines for earthquake research (Reches *et al.*, 2006). The central part of this project is dense instrumentation and detailed characterization of a large fault zone in TauTona mine, which is the deepest mine on Earth (approaching 4 km, depth) located within the Western Deep Levels of the Witwatersrand basin, South Africa (**Figure 11**).

The laboratory is built around the Pretorius Fault Zone (shown in pink in the lower part of **Figure 11**), which is at least 10 km long with 30–200 m of displacement and which appears to have been inactive for the past 2.5 Ga. The mining plan for the next few years is likely to induce earthquakes of significant magnitude ($M > 2$) along this fault. NELSAM science activities at the site started in 2005 with site characterization, including mapping of 3D structure and composition of the Pretorius fault zones at 3.54 km depth. The emphasis of the investigations has been on segments of the fault zone that were reactivated during recent earthquakes. Analysis of the stress state both near and away from the excavation will be carried out using techniques developed for the oil industry in which compressive and tensile wellbore failures are studied in wells of different orientation (e.g., Zoback *et al.*, 2003). In addition, five boreholes, 20–60 m in length, have been drilled across the Pretorius Fault Zone. Once completed, the earthquake laboratory will include a dense array (250 m footprint) of three-component broadband accelerometers, seismometers, strain meters, temperature sensors, creep meters, electromagnetic radiation sensors, and acoustic emissions sensors. Fault-zone fluid chemistry will be monitored with an onsite mass spectrometer.

A M 2.2 earthquake that occurred on 12 December 2004 in the center of the planned earthquake laboratory that reactivated several segments of the Pretorius Fault (Heesakkers *et al.*, 2005). The mapping of the rupture zone of this earthquake in three dimensions revealed quasi-planar, cross-cutting reactivated segments with inclinations ranging from 21° to 90°. The rupturing

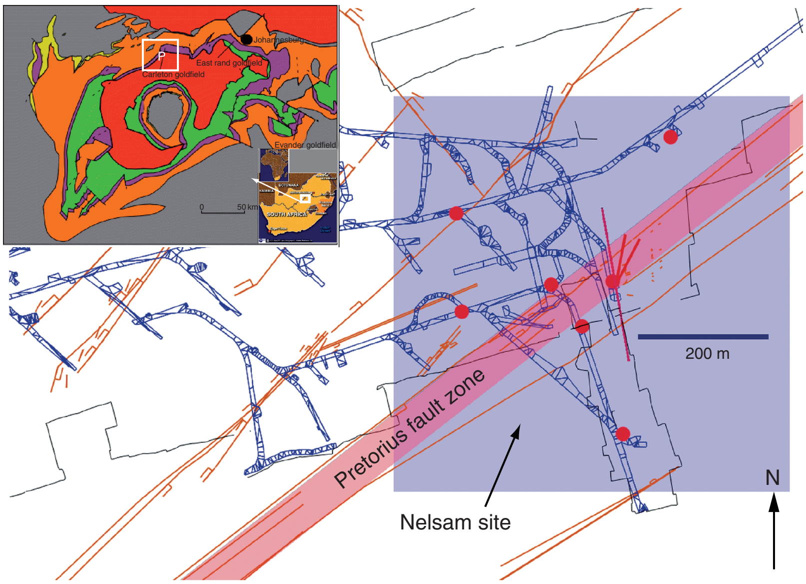

Figure 11 The TauTona mine is located in the Carleton goldfield, approximately 80 km west of Johannesburg, South Africa (see inset). Scientific drilling is occurring in the vicinity of the Pretorius Fault Zone (shown by pink shading) where a number of recent earthquakes have occurred recently. The figure shows the excavations at a depth of 3597–3657 m. Most of the faults exposed in the mine tunnels trend NE–SW, similar to the overall trend of the Pretorius Fault Zone. Courtesy of Z. Reches.

formed fresh fine-grained white rock powder almost exclusively along the contacts of the ancient, sintered cataclasite, and the quartzitic host rock.

4.22.5.11 NanTroSeize

An extensive fault-zone drilling campaign is planed as part of NanTroSeize experiment (**Figure 12(a)**) to be carried out by the Integrated Ocean Drilling Program in the Nankai trough just off southern Honshu, Japan. The extent of the 1944 Tonankai earthquake slip zone, the presumed extent of the locked zone (indicated by the heavy white line), and the presumed seismogenic zone are also shown.

The first-order objectives are to:

- document the material properties and state of the plate boundary fault system at several *P*–*T* and

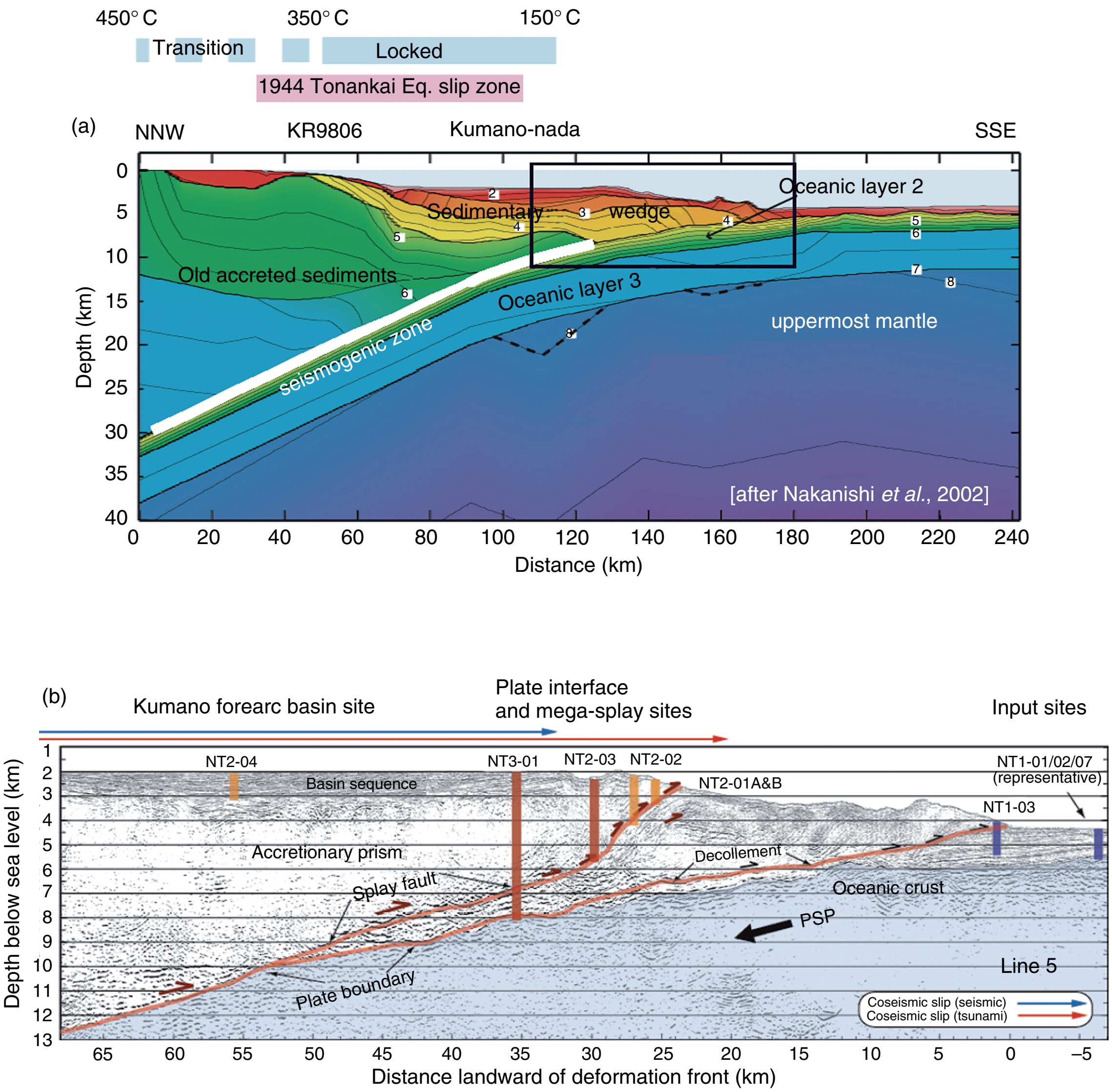

Figure 12 (a) Seismic velocity structure in the Nankai trough area reveals the nature of the downgoing Philippine Sea plate, the accretionary wedge and old accreted sediments (after Nakanishi *et al.*, 2002). The extent of the 1944 Tonankai earthquake slip zone, the presumed extent of the locked zone (indicated by the heavy white line) and the presumed seismogenic zone are also shown. (b) A detailed view of the proposed drilling area (see box in (a) where seismic reflection data reveals the detailed structure of the main décollement and splay faults in the accreationary prism). Note that a series of boreholes are planned to penetrate various parts of the main décollement and splay faults. Courtesy of H. Tobin.

lithology conditions, testing hypotheses for stable versus unstable frictional behavior;
- investigate partitioning between seismic versus aseismic processes on the main plate boundary, through monitoring of seismicity, borehole strain, and pore fluid pressure;
- test whether there are interseismic temporal changes in state along the plate-boundary thrust, including possible earthquake precursory signals; and
- use downhole measurements and sampling to calibrate observations made in the broader geophysical volume surrounding the boreholes.

In many ways, the specific science goals of this experiment are somewhat similar to those of the SAFOD project, although in a much different geologic setting. Specifically, the goals are to

- obtain samples of faults and surrounding environment
  - characterize lithology, structure, elastic and mechanical properties, porosity, permeability, pore fluid chemistry, microbiology;
  - use familiar ODP coring techniques, augmented by cuttings and sidewall coring;
- characterize the near-borehole environment;
  - geophysical logging: wireline and Logging While Drilling (LWD);
  - active testing for pore fluid pressure, stress, hydrogeologic properties (permeability, storage);
- monitor the borehole environment over time
  - passive and active source seismology;
  - strain and tilt;
  - pore fluid pressure;
  - temperature; and
  - EM field.

A detailed view of the proposed drilling area is shown in **Figure 12(b)** (see box in **Figure 12(a)**) where seismic reflection data reveal the detailed structure of the main décollement and splay faults in the accreationary prism. As shown, a series of relatively shallow holes will be drilled through splay faults in the accretionary wedge to study aseismic faulting. Following drilling, these holes will be used for downhole observatories. An eventual ultradeep borehole to be drilled into a seismogenic section of the décollement and possibly seismogenic deep part of the splay fault.

4.22.6 Summary

Drilling and downhole measurements in active fault zones provide critical tests of hypotheses arising from seismologic observations, laboratory rock deformation experiments, and geological observations of exhumed fault zones. Drilling provides the only direct means of measuring pore pressure, stress, permeability, and other important parameters within and near an active fault zone at depth. It is also the only way to collect fluid and rock samples from the fault zone and wall rocks at seismogenic depths and to monitor time-dependent changes in fluid pressure, fluid chemistry, deformation, temperature and electromagnetic properties at depth during the earthquake cycle. In the context of the processes and properties alluded to above, *in situ* observations and sampling through drilling perform two critical, and unique, functions. Sampling of fault rocks and fluids and downhole measurements provide essential constraints on mineralogy, grain size, fluid chemistry, temperature, stress, pore geometry, and other parameters that would allow laboratory investigations of fault-zone rheology and frictional behavior to be conducted under realistic *in situ* conditions. By *in situ* sampling, downhole measurement, and long-term monitoring in active fault zones, one is able to test and refine the broad range of current theoretical models for faulting and seismogenesis by providing realistic constraints on fault-zone physical properties, loading conditions, and mechanical behavior at depth. In particular, by comparing results of microstructural observations and rheological investigations on core with measurements of microseismicity, fluid pressure and deformation during the fault-zone monitoring phase of this experiment, we would be able to differentiate between fault-zone processes (e.g., fluid pressure fluctuations) associated with fault creep versus earthquakes.

Of course, no single drill hole into an active fault can address all of the questions listed above. Rather, like other avenues of earthquake research, the experiments being carried out in fault-related scientific drilling projects around the world (such as the ones noted above) cumulatively address many critical scientific questions about fault-zone structure, composition, and processes. Over time, the accumulation of data from these experiments will result in important advances in earthquake science.

References

Abercrombie RE (1995) Earthquake source scaling relationships from -1 to 5 M_1 using seismograms recorded at 2.5 km depth. *Journal of Geophysical Research* 100: 24015–24036.

Abercrombie RE and Leary P (1993) Source parameters of small earthquakes recorded at 2.5 km depth, Cajon pass, Southern California: Implications for earthquake scaling. *Geophysical Research Letters* 20: 1511–1514.

Ando M (2001) Geological and geophysical studies of the Nojima Fault from drilling: An outline of the Nojima Fault Zone Probe. *The Island Arc* 10: 206–214.

Andreani M, Boullier A-M, and Gratier J-P (2005) Development of schistosity by dissolution–crystallization in a California serpentinite gouge. *Journal of Structural Geology* 27: 2256–2267.

Andrews D (2002) A fluid constitutive relation accounting for thermal pressurization of pore fluid. *Journal of Geophysical Research* 107(B12): 2363 (doi:10.1029/2002JB001942).

Andrews DJ and Ben-Zion Y (1997) Wrinkle-like slip pulse on a fault between different materials. *Journal of Geophysical Research* 102: 553–571.

Angevine CL, Turcotte DL, and Furnish MD (1982) Pressure solution lithification as a mechanism for the stick-slip behavior of faults. *Tectonics* 1: 151–160.

Anooshehpoor A and Brune JN (1994) Frictional heat generation and seismic radiation in a foam rubber model of earthquakes. *Pure and Applied Geophysics* 142: 735–748.

Bangs NL, Shipley TH, Gulick SPS, Moore G, Kuromoto S, and Nakamura Y (2004) Evolution of the Nankai Trough decollement from the trench into the seismogenic zone; inferences from three-dimensional seismic reflection imaging. *Geology* 32: 273–276.

Barton CA, Zoback MD, and Burns KL (1988) *In-situ* stress orientation and magnitude at the Fenton Geothermal site, New Mexico, determined from wellbore breakouts. *Geophysical Research Letters* 15: 467–470.

Baumgärtner J and Zoback MD (1989) Interpretation of hydraulic fracturing pressure–time records using interactive analysis methods. *International Journal of Rock Mechanics, Mining Science and Geomechanical Abstracts* 26: 461–470.

Ben-Avraham Z and Zoback MD (1992) Transform-normal extension and asymmetric basins: An alternative to pull-apart models. *Geology* 20: 423–426.

Beroza GC and Ellsworth WL (1996) Properties of the seismic nucleation phase. *Tectonophysics* 261: 209–227.

Bird P (1984) Hydration-phase diagrams and friction of montmorillonite under laboratory and geologic conditions, with implications for shale compaction, slope stability, and strength of fault gouge. *Tectonophysics* 107: 235–260.

Blanpied ML, Lockner DA, and Byerlee JD (1991) Fault stability inferred from granite sliding experiments at hydrothermal conditions. *Geophysical Research Letters* 18: 609–612.

Boness N and Zoback MD (2006) A multi-scale study of the mechanisms controlling shear velocity anisotropy in the San Andreas Fault Observatory at Depth. *Geophysics* 7(5): F131–F146.

Bos B and Spiers CJ (2001) Experimental investigation into the microstructural and mechanical evolution of phyllosilicate-bearing fault rock under conditions favouring pressure solution. *Journal of Structural Geology* 23: 1187–1202.

Boullier A-M, Ohtani T, Fujimoto K, Ito H, and Dubois M (2001) Fluid inclusions in pseudotachylytes from the Nojima fault, Japan. *Journal of Geophysical Research* 106(B10): 21965–21978 (doi:10.1029/2000JB000043).

Boullier A-M and Robert F (1992) Paleoseismic events recorded in Archaean gold-quartz vein networks, Val d'Or, Albitibi, Quebec, Canada. *Journal of Structural Geology* 14: 161–179.

Brace WF and Kohlstedt DL (1980) Limits on lithospheric stress imposed by laboratory experiments. *Journal of Geophysical Research* 85: 6248–6252.

Brodsky EE and Kanamori H (2001) The elastohydrodynamic lubrication of faults. *Journal of Geophysical Research* 106: 16357–16374.

Brudy M, Zoback MD, Fuchs K, Rummel F, and Baumgärtner J (1997) Estimation of the complete stress tensor to 8 km depth in the KTB scientific drill holes: Implications for crustal strength. *Journal of Geophysical Research* 102: 18453–18475.

Bruhn RL, Parry WT, Yonkee WA, and Thompson T (1994) Fracturing and hydrothermal alteration in normal fault zones. *Pure and Applied Geophysics* 142: 609–644.

Bruhn RL, Yonkee WA, and Parry WT (1990) Structural and fluid-chemical properties of seismogenic normal faults. *Tectonophysics* 175: 139–157.

Brune JN (1970) Tectonic stress and the spectra of seismic shear waves from earthquakes. *Journal of Geophysical Research* 75: 4997–5009.

Brune JN, Brown S, and Johnson PA (1993) Rupture mechanism and interface separation in foam rubber models of earthquakes: A possible solution to the heat flow paradox and the paradox of large overthrusts. *Tectonophysics* 218: 59–67.

Brune JN, Henyey TL, and Roy RF (1969) Heat flow, stress, and rate of slip along the San Andreas fault, California. *Journal of Geophysical Research* 74: 3821–3827.

Burford RO and Harsh PW (1980) Slip on the San Andreas fault in central California from alinement array surveys. *Bulletin of the Seismological Society of America* 70: 1233–1261.

Byerlee JD (1978) Friction of rocks. *Pure and Applied Geophysics* 116: 615–629.

Byerlee JD (1990) Friction, overpressure and fault normal compression. *Geophysical Research Letters* 17: 2109–2112.

Byerlee JD (1993) A model for episodic flow of high pressure water in fault zones before earthquakes. *Geology* 21: 303–306.

Byerlee JD and Summers R (1976) A note on the effect of fault gouge thickness on fault stability. *International Journal of Rock Mechanics, Mining Science and Geomechanical Abstracts* 13: 35–36.

Byrne T and Fisher D (1990) Evidence for a weak and overpressured décollement beneath sediment-dominated accretionary prisms. *Journal of Geophysical Research* 98: 9081–9097.

Chester FM, Evans JP, and Biegel RL (1993) Internal structure and weakening mechanisms of the San Andreas fault. *Journal of Geophysical Research* 98: 771–786.

Chester FM and Higgs NG (1992) Multimechanism friction constitutive model for ultrafine quartz gouge at hypocentral conditions. *Journal of Geophysical Research* 97: 1859–1870.

Cornet FH, Bernard P, and Moretti I (2004) The Corinth Rift Laboratory. *Comptes Rendus Geosciences* 336: 235–241.

Dahlen FA (1990) Critical taper model of fold-and-thrust belts and accretionary wedges. *Annual Review of Earth and Planetary Sciences* 18: 55–99.

Davis D, Suppe J, and Dahlen FA (1983) The mechanics of fold and thrust belts and accretionary wedges. *Journal of Geophysical Research* 88: 1153–1172.

Dewers T and Ortoleva P (1994) Nonlinear dynamical aspects of deep basin hydrology; fluid compartment formation and episodic fluid release. *American Journal of Science* 294: 713–755.

Dreger DS, Tkalcic H, and Johnston M (2000) Dilational processes accompanying earthquakes in the Long Valley Caldera. *Science* 288: 122–125.

Dieterich JH (1992) Earthquake nucleation on faults with rate- and state-dependent strength. *Tectonophysics* 211: 115–134.

Eichhubl P and Boles JR (2000) Rates of fluid flow in fault systems – Evidence for episodic rapid fluid flow in the Miocene Monterey Formation Coastal California. *American Journal of Science* 300: 571–600.

Ellsworth WL and Beroza GC (1995) Seismic evidence for an earthquake nucleation phase. *Science* 268: 851–855.

Ellsworth WL and Beroza GC (1998) Observation of the seismic nucleation phase in the Ridgecrest, California earthquake sequence. *Geophysical Research Letters* 25: 401–404.

Evans JP and Chester FM (1995) Fluid-rock interaction in rocks of the San Andreas system: Inferences from San Gabriel fault rock geochemistry and microstructures. *Journal of Geophysical Research* 100: 13007–13020.

Fehler MC (1989) Stress control of seismicity patterns observed during hydraulic fracturing experiments at the Fenton Hill hot dry rock geothermal energy site, New Mexico. *International Journal of Rock Mechanics and Mining Sciences* 26: 211–219.

Fisher DM (1996) Fabrics and veins in the forearc: A record of cyclic fluid flow at depths of <15 km. In: Bebout GE, Schou DW, Kirby SH, and Platt JJ (eds.) *American Geophysical Union Geophysical Monograph, Vol. 96: Subduction: Top to Bottom*, pp. 75–89. Washington, DC: American Geophysical Union.

Fitzenz DD and Miller SA (2003) Fault compaction and overpressured faults: Results from a 3D model of a ductile fault zone. *Geophysical Journal International* 155: 111–125.

Flesch LM, Holt WE, Haines AJ, and Shen-Tu B (2000) Dynamics of the Pacific-North American plate boundary in the Western United States. *Science* 287: 834–836.

Fournier RL (1996) Compressive and tensile failure at high fluid pressure where preexisting fractures have cohesive strength, with application to the San Andreas fault. *Journal of Geophysical Research* 101: 25499–25509.

Fujimoto K, Tanaka H, Higuchi T, Tomida N, Ohtani T, and Ito H (2001) Alteration and mass transfer inferred from the Hirabayashi GSJ drill penetrating the Nojima fault, Japan. *The Island Arc* 10: 401–410.

Fyfe S, Price NJ, and Thomson AB (1978) *Fluids in the Earth's Crust*. New York: Elsevier.

Hacker BR, Blanpied ML, Lockner DA, and Jové CF (1995) Dehydration and friction: Laumontite -> wairakite + H_2O. *Geological Society of America, Abstracts with Programs* 27: A282.

Hainzl S and Ogata Y (2005) Detecting fluid signals in seismicity data through statistical earthquake modeling. *Journal of Geophysical Research* 110: B05S07 (doi:10.1029/2004JB003247).

Harris RA (1998) Introduction to special section: Stress triggers, stress shadows and implications for seismic hazard. *Journal of Geophysical Research* 103: 24347–24358.

Harris RA (2004) Numerical simulations of large earthquakes: Dynamic rupture propagation on heterogeneous faults. *Pure and Applied Geophysics* 161: 2171–2181 (doi:10.1007/s00024-004-2556-8).

Healy JH, Rubey WW, Griggs DT, and Raleigh CB (1968) The Denver earthquakes. *Science* 161: 1301–1310.

Heaton TH (1990) Evidence for and implications of self-healing pulses of slip in earthquake rupture. *Physics of the Earth and Planetary Interiors* 64: 1–20.

Heesakkers V, Murphy SK, van Aswegen G, *et al.* (2005) The rupture zone of the M = 2.2 earthquake that reactivated the ancient Pretorius Fault in TauTona Mine, South Africa. *EOS Transactions of the American Geophysical Union* 86: S31B-04.

Henyey TL and Wasserburg GJ (1971) Heat flow near major strike-slip faults in California. *Journal of Geophysical Research* 76: 7924–7946.

Hickman S (1991) Stress in the lithosphere and the strength of active faults, US National Report on International Union of Geodesy and Geophysics 1987–1990. *Reviews of Geophysics* 29: 759–775.

Hickman S, Barton CA, Zoback MD, Morin R, Sass J, and Benoit R (1997) *In-situ* stress and fracture permeability along the Stillwater fault zone, Dixie Valley, Nevada. *International Journal of Rock Mechanics and Mining Sciences* 34: 3–4 (Paper No. 126).

Hickman S and Evans B (1992) Growth of grain contacts in halite by solution transfer: Implications for diagenesis, lithification, and strength recovery. In: Evans B and Wong T-F (eds.) *Fault Mechanics and Transport Properties of Rocks*, pp. 253–280. San Diego, CA: Academic Press.

Hickman S, Sibson R, and Bruhn R (1995) Introduction to special section: Mechanical involvement of fluids in faulting. *Journal of Geophysical Research* 100: 12831–12840.

Hickman S and Zoback MD (2004) Stress measurements in the SAFOD pilot hole: Implications for the frictional strength of the San Andreas fault. *Geophysical Research Letters* 31: L15S12.

Hickman S, Zoback MD, and Ellsworth WE (2004) Introduction to special section: Preparing for the San Andreas Fault Observatory at Depth. *Geophysical Research Letters* 31: L12S01 (doi:10.1029/20040GL20688).

Hubbert MK and Rubey WW (1959) Role of fluid pressure in mechanics of overthrust faulting. *Geological Society of America, Bulletin* 70: 115–205.

Hunt JM (1990) Generation and migration of petroleum from abnormally pressured fluid compartments. *American Association of Petroleum Geologists Bulletin* 74: 1–12.

Iio Y (1992) Slow initial phase of the S-wave velocity pulse generated by microearthquakes. *Geophysical Research Letters* 19: 477–480.

Iio Y (1995) Observation of the slow initial phase of microearthquakes implications for earthquake nucleation and propagation. *Journal of Geophysical Research* 100: 15333–15349.

Imanishi K, Ellsworth WE, and Prejean SG (2004) Earthquake source parameters etermined by the SAFOD pilot hole array. *Geophysical Research Letters* 31: L12S09 (doi:10.1029/2004GL019420).

Imanishi K and Ellsworth WL (2006) Source scaling relationships of microearthquakes at Parkfield, CA, determined using the SAFOD pilot hole seismic array. In: McGarr A, Kanamori H, and Abercrombie R (eds.) *AGU Monograph on Radiated Energy and the Physics of Earthquake Faulting*. Geophysical Monograph Series 170, pp. 81–90. American Geophysical Union.

Janecke SU and Evans JP (1988) Feldspar-influenced rock rheologies. *Geology* 16: 1064–1067.

Kanamori H (1980) State of stress in the Earth's lithosphere. In: Dziewonski AM and Boschi E (eds.) *Physics of the Earth's Interior*, pp. 531–554. Bologna, Italy: Societá Italiana di Fisica.

Kano H, Mori J, Fujio R, *et al.* (2006) Heat signature of the Chelungpu fault associated with the 1999 Chi-chi Taiwan earthquake. *Geophysical Research Letters* 33: L14306.

Kao H and Angelier J (2001) Stress tensor inversion for the Chi-chi earthquake sequence and its implications on regional collision. *Bulletin of the Seismological Society of America* 91: 1028–1040.

Karner S, Marone C, and Evans B (1997) Laboratory study of fault healing and lithification in simulated fault gouge under hydrothermal conditions. *Tectonophysics* 277: 41–55.

Kennedy BM, Kharaka YH, Evans WC, *et al.* (1997) Mantle fluids in the San Andreas fault system, California. *Science* 278: 1278–1281.
Kerrich R, La Tour TE, and Willmore L (1984) Fluid participation in deep fault zones: Evidence from geological, geochemical, and $^{18}O/^{16}O$ relations. *Journal of Geophysical Research* 89: 4331–4343.
Kirby SH (1983) Rheology of the lithosphere. *Reviews of Geophysics and Space Physics 21:* 1458–1487.
Ko S-Z, Olgaard DL, and Wong T-F (1997) Generation and maintenance of pore presure excess in a dehydrating system 1. Experimental and microstructural observations. *Journal of Geophysical Research* 102: 825–839.
Kostrov BV (1964) Self-similar problem of propagation of shear cracks. *Journal of Applied Mathematics and Mechanics* 28: 1077–1087.
Lachenbruch AH (1980) Frictional heating, fluid pressure, and the resistance to fault motion. *Journal of Geophysical Research* 85: 6097–6112.
Lachenbruch AH and McGarr A (1990) Stress and heat flow. In: Wallace RE (ed.) *US Geological Survey Professional Paper 1515: The San Andreas Fault System, California*, pp. 261–277. Menlo Park, CA: USGS.
Lachenbruch AH and Sass JH (1980) Heat flow and energetics of the San Andreas fault zone. *Journal of Geophysical Research* 85: 6185–6223.
Lachenbruch AH and Sass JH (1992) Heat flow from Cajon Pass, fault strength and tectonic implications. *Journal of Geophysical Research* 97: 4995–5015.
Lachenbruch AH and Thompson GA (1972) Oceanic ridges and transform faults: Their intersection angles and resistance to place motion. *Earth and Planetary Science Letters* 15: 116–122.
Lockner DA and Byerlee JD (1995) An earthquake instability model based on faults containing high fluid-pressure compartments. *Pure and Applied Geophysics* 145: 717–745.
Logan JM and Rauenzahn KA (1987) Frictional dependence of gouge mixtures of quartz and montmorillonite on velocity, composition and fabric. *Tectonophysics* 144: 87–108.
Lund B and Zoback MD (1999) State of stress to 7 km depth in the Siljan drill holes from observations of drilling-induced tensile wall fractures. *International Journal of Rock Mechanics* 36: 169–190.
Ma K-F, Brodsky EE, Mori J, Song C, Ji TR, and Kanamori H (2003) Evidence for fault lubrication during the 1999 Chi-Chi, Taiwan, earthquake (Mw 7.6). *Geophysical Research letters* 30: 1244 (doi:10.1029/2002GL015380).
Ma K-F, Tanaka H, Song S-R, *et al.* (2006) Slip zone and energetics of a large earthquake from the Taiwan Chelungpu-fault Drilling Project. *Nature* 444: 473–476.
Madariaga R (1976) Dynamics of an expanding circular fault. *Bulletin of the Seismological Society of America* 66: 639–666.
Magee ME and Zoback MD (1993) Evidence for a weak interpolate thrust fault along the northern Japan subduction zone and implications for the mechanics of thrust faulting and fluid expulsion. *Geology* 21: 809–812.
Marone C, Raleigh CB, and Scholz CH (1990) Frictional behavior and constitutive modeling of simulated fault gouge. *Journal of Geophysical Research* 95: 7007–7025.
Mase CW and Smith L (1987) Effects of frictional heating on the thermal, hydrological, and mechanical response of a fault. *Journal of Geophysical Research* 92: 6249–6272.
Martinsen RS (1997) Stratigraphic controls on the development and distribution of fluid-pressure compartments. *American Association of Petroleum Geologists Memoir* 67: 223–241.
McNutt M (1980) Implications of regional gravity for state of stress in the Earth's crust and upper mantle. *Journal of Geophysical Research* 85: 6377–6396.
McNutt MK and Menard HW (1982) Constraints on yield strength in the oceanic lithosphere derived from observations of flexure. *Geophysical Journal of the Royal Astronomical Society* 71: 363–394.
Melosh HJ (1979) Acoustic fluidization: A new geologic process?. *Journal of Geophysical Research* 84: 7513–7520.
Melosh HJ (1996) Dynamic weakening of faults by acoustic fluidization. *Nature* 379: 601–606.
Miller SA (1996) Fluid-mediated influence of adjacent thrusting on the seismic cycle at Parkfield. *Nature* 382: 799–802.
Moore DE, Lockner DA, Summers R, Shengli M, and Byerlee JD (1997) Strengths of serpentinite gouges at elevated temperatures. *Journal of Geophysical Research* 102: 14787–14801.
Moore JC, Shipley TH, Goldberg D, *et al.* (1995) Abnormal fluid pressure and fault-zone dilation in the Barbados acretionary prism: Evidence from logging while drilling. *Geology* 23: 605–608.
Moore JC and Vrolijk P (1992) Fluids in accretionary prisms. *Reviews of Geophysics* 30: 113–135.
Morrow CA, Shi LQ, and Byerlee JD (1982) Strain hardening and strength of clay-rich fault gouges. *Journal of Geophysical Research* 87: 6771–6780.
Morrow C, Radney B, and Byerlee J (1992) Frictional strength and the effective pressure law of montmorillonite and illite clays. In: Evans B and Wong T-F (eds.) *Fault Mechanics and Transport Properties of Rocks*, pp. 69–88. San Diego, CA: Academic Press.
Mount VS and Suppe J (1987) State of stress near the San Andreas fault: Implications for wrench tectonics. *Geology* 15: 1143–1146.
Mount VS and Suppe J (1992) Present-day stress orientations adjacent to active strike-slip faults: California and Sumatra. *Journal of Geophysical Research* 97: 11995–12013.
Mrotek KA, Quittmeyer RC, Naumhoff PG, and Stratton CT (1988) Observations of the earthquake swarm near Moodus, Connecticut. September/October, 1987. *EOS Transactions of the American Geophysical Union* 69: 495.
Murray MH and Segall P (2001) Modeling broadscale deformation in northern California and Nevada from plate motions and elastic strain accumulation. *Geophysical Research Letters* 28(22): 4315–4318.
Nadeau R, Antolik M, Johnson P, Foxall W, and McEvilly TV (1994) Seismological studies at Parkfield III: Microearthquake clusters in the study of fault-zone dynamics. *Bulletin of the Seismological Society of America* 84: 247–263.
Nadeau RM and McEvilly TV (1997) Seismological studies at Parkfield V: Characteristic microearthquake sequences as fault-zone drilling targets. *Bulletin of the Seismological Society of America* 87: 1463–1472.
Nadeau RM, Foxall W, and McEvilly TV (1995) Clustering and periodic recurrence of microearthquakes on the San Andreas fault at Parkfield, California. *Science* 267: 503–507.
Nadeau RM, Michelini A, Uhrhammer RA, Dolenc D, and McEvilly TV (2004) Detailed kinematics, structure and recurrence of micro-seismicity in the SAFOD target region. *Geophysical Research Letters* 31: L12S08 (doi:10.1029/2003GL019409).
Nakanishi A, Takahashi N, Park J-O, *et al.* (2002) Crustal structure across the coseismic rupture zone of the 1944 Tonankai earthquake, the central Nanki Trough seismogenic zone. *Geophysical Research* 107: doi:10.1029/2001JB00424.
Nur A and Booker JR (1972) Aftershocks caused by pore-fluid flow? *Science* 175: 885–887.
Ohnaka M (1992) Earthquake source nucleation: A physical model for short-term precursors. *Tectonophysics* 211: 149–178.

Ohtani T, Tanaka H, Fujimoto K, Higuchi T, Tomida N, and Ito H (2001) Internal structure of the Nojima fault zone from the Hirabayashi GSJ drill core. *The Island Arc* 10: 392–400.
Oppenheimer DH, Reasenberg PA, and Simpson RW (1988) Fault-plane solutions for the 1984 Morgan Hill, California earthquake sequence: Evidence for the state of stress on the Calaveras fault. *Journal of Geophysical Research* 93: 9007–9026.
Oshiman N, Shimamoto T, Takemura K, and Wibberley CAJ eds. (2001) Nojima Fault Zone probe. *The Island Arc* 10: 195–505.
Parry WT (1994) Fault fluid compositions from fluid inclusion observations. In: Hickman S, Sibson R, and Bruhn R (eds.) *Proceedings USGS Red Book Conference on the Mechanical Involvement of Fluids in Faulting*, pp. 334–348. Menlo Park, CA: USGS.
Peyrat S, Olsen KB, and Madariaga R (2004) Which dynamic rupture parameters can be estimated from strong ground motion and geodetic data? *Pure and Applied Geophysics* 161: 2155–2169 (doi:10.1007/s00024-004-2555-9).
Pinkston J, Stern L, and Kirby S (1987) Hydrothermal reactions on artificial fault surfaces in dunite: Fibrous mineral growth, slickensides and temperature sensitivity of reaction weakening. *EOS Transactions of the American Geophysical Union* 68: 405.
Power WL and Tullis TE (1989) The relationship between slickenside surfaces in fine-grained quartz and the seismic cycle. *Journal of Structural Geology* 11: 879–893.
Powley DE (1990) Pressures and hydrogeology in petroleum basins. *Earth, Science Reviews* 29: 215–226.
Prejean SG and Ellsworth WL (2001) Observations of earthquake source parameters at 2 km depth in the Long Valley Caldera, Eastern California. *EOS Transactions of the American Geophysical Union* 91: 165–177.
Raleigh CB, Healy JH, and Bredehoeft JD (1972) An experiment in earthquake control at Rangely, Colorado. *Science* 191: 1230–1237.
Reches Z, DAFSAM, and NELSAM teams (2006) Building a natural earthquake laboratory at focal depth (DAFSAM-NELSAM Project, South Africa). *Scientific Drilling* 3: 30–33.
Reinen LA and Tullis TE (1995) Microstructural evidence of strain localization and distributed strain in serpentine friction experiments. *EOS Transactions of the American Geophysical Union* 76: F560.
Reinen LA, Weeks JD, and Tullis TE (1994) The frictional behavior of lizardite and antigorite sepentinites: Experiments, constitutive models, and implications for natural faults. *Pure and Applied Geophysics* 143: 317–358.
Rice JR (1992) Fault stress states, pore pressure distributions, and the weakness of the San Andreas fault. In: Evans B and Wong T-F (eds.) *Fault Mechanics and Transport Properties of Rocks*, pp. 475–503. San Diego, CA: Academic Press.
Rice JR (2006) Heating and weakening of faults during earthquake slip. *Journal of Geophysical Research* 111: B05311 (doi:10.1029/2005JB004006, 29 pages).
Rice JR and Cleary MP (1976) Some basic stress diffusion solutions for fluid-saturated elastic porous media with compressible constituents. *Reviews of Geophysics* 14: 227–241.
Rudnicki J (1988) Physical models of earthquake instability and precursory processes. *Pure and Applied Geophysics* 126: 524–531.
Rutter EH and Mainprice DH (1979) On the possibility of slow fault slip controlled by diffusive mass transfer processes. *Gerlands Beitrage zur Geophysik* 88: 154–162.
Saffer DM and Bekins BA (2006) An evaluation of factors influencing pore pressure in accretionary complexes: Implications for taper angle and wedge mechanics. *Journal of Geophysical Research* 111: B04101 (doi:10.1029/2005JB003990).
Saffer DM, Bekins BA, and Hickman S (2003) Topographically driven groundwater flow and the San Andreas heat flow paradox revisited. *Journal of Geophysical Research* 108(B5): 2274.
Scholz CH (1989) Mechanics of faulting. *Annual Review of Earth and Planetary Sciences* 17: 309–334.
Scholz CH (2000) Evidence for a strong San Andreas fault. *Geology* 28(2): 163–166.
Schulz SE and Evans JP (2000) Mesoscopic structure of the Punchbowl fault, southern California and the geologic and geophysical structure of active strike-slip faults. *Journal of Structural Geology* 22: 913–930.
Schulz SS (1989) Catalog of creepmeter measurements in California from 1966 through 1988. *US Geological Survey Open-File Report 89–650*. Menlo Park, CA: USGC.
Segall P and Rice JR (1995) Dilatancy, compaction and slip instability of a fluid-infiltrated fault. *Journal of Geophysical Research* 100: 22155–22171.
Shimamoto T and Logan J (1981) Effects of simulated clay gouges on the sliding behavior of Tennessee sandstone. *Tectonophysics* 75: 243–255.
Shipley TH, Moore GF, Bangs NL, Moore JC, and Stoffa PL (1994) Seismically inferred dilatancy distribution, northern Barbados Ridge decollement: Implications for fluid migration and fault strength. *Geology* 22: 411–414.
Sibson RH (1973) Interactions between temperature and pore-fluid pressure during earthquake faulting: A mechanism for partial or total stress relief. *Nature, Physical Science* 243: 66–68.
Sibson RH (1985) Stopping of earthquake ruptures at dilational fault jogs. *Nature* 316: 248–251.
Sibson RH (1990) Rupture nucleation on unfavorably oriented faults. *Bulletin of the Seismological Society of America* 80: 1580–1604.
Sleep NH (1995) Ductile creep, compaction and rate and state dependent friction within major fault zones. *Journal of Geophysical Research* 100: 13065–13080.
Sleep NH and Blanpied ML (1992) Creep, compaction, and the weak rheology of major faults. *Nature* 359: 687–692.
Sleep NH and Blanpied ML (1994) Ductile creep and compaction: A mechanism for transiently increasing fluid pressure in mostly sealed fault zones. *Pure and Applied Geophysics* 143: 9–40.
Smith L, Forster CB and Evans JP (1990) Interaction of fault zones, fluid flow and heat transfer on a basin scale. In: Newman SP and Neretnieks I (eds.) *Hydrogeology of Low Permeability Environments*. International Association of Hydrological Sciences, Selected Papers, 2, pp. 41–67.
Spray JG (1987) Artificial generation of pseudotachylite using friction welding apparatus: Simulation of melting on a fault plane. *Journal of Structural Geology* 9: 49–60.
Stock JM, Healy JH, Hickman SH, and Zoback MD (1985) Hydraulic fracturing stress measurements at Yucca Mountain, Nevada, and relationship to regional stress field. *Journal of Geophysical Research* 90: 8691–8706.
Tanaka H, Chen WM, Kawabata K, and Urata N (2007) Thermal properties across the Chelungpu fault zone and evaluations of positive thermal anomaly on the slip zones: Are these residuals of heat from faulting. *Geophysical Research Letters* 34: L1309.
Tanaka H, Kujimoto K, Ohtani T, and Ito H (2001) Structural and chemical characterization of shear zones in the freshly activated Nojima fault, Awaji Island, southwest Japan. *Journal of Geophysical Research* 106: 8789–8810.
Tanaka H, Wang CY, Chen WM, *et al.* (2002) Initial science report of shallow drilling penetrating into the Chelungpu fault zone, Taiwan. *Terrestrial, Atmospheric and Oceanic Sciences* 13: 227–251.
Townend J and Zoback MD (2000) How faulting keeps the crust strong. *Geology* 28(5): 399–402.

Townend J and Zoback MD (2004) Regional tectonic stress near the San Andreas fault in Central and Northern California. *Geophysical Research Letters* 31(13): L15S11.
Townend J and Zoback MD (2001) Implications of earthquake focal mechanisms for the frictional strength of the San Andreas fault system. In: Holdsworth RE, Strachan RA, Macloughlin JJ, and Knipe RJ (eds.) *Special Publication of the Geological Society of London, Vol. 186: The Nature and Tectonic Significance of Fault Zone Weakening*, pp. 13–21. Geological Society of London: London.
Wald DJ and Heaton TH (1994) Spatial and temporal distribution of slip for the 1992 Landers, California, earthquake. *Bulletin of the Seismological Society of America* 84: 668–691.
Wakita H and Sano Y (1987) High 3He emanation and seismic swarms observed in a nonvolcanic, forearc region. *Journal of Geophysical Research* 92: 12539–12546.
Wang CY, Mao N, and Wu FT (1980) Mechanical properties of clays at high pressure. *Journal of Geophysical Research* 85: 1462–1468.
Wang K, Mulder T, Rogers G, and Hyndman R (1995) Case for very low coupling stress on the Cascadia subduction fault. *Journal of Geophysical Research* 100: 12907–12918.
Wilcock WSD, Purdy GM, and Solomon SC (1990) Microearthquake evidence for extension across the Kane transform fault. *Journal of Geophysical Research* 95: 15439–15462.
Williams CF, Grubb FV, and Galanis SP (2004) Heat flow in the SAFOD pilot hole and implications for the strength of the San Andreas Fault. *Geophysical Research Letters* 31: L15S14 (doi:10.1029/2003GL019352).
Wintsch R, Christoffersen R, and Kronenberg A (1995) Fluid-rock reaction weakening of fault zones. *Journal of Geophysical Research* 100: 13021–13032.
Wu FT (1978) Mineralogy and physical nature of clay gouge. *Pure and Applied Geophysics* 116: 655–689.
Wu H-Y, Ma K-F, Zoback M, Boness N, Ito H, and Hung J-H (2007) Stress orientations of Taiwan Chelungpu-Fault Drilling Project (TCDP) hole-A as observed from geophysical logs. *Geophysical Research Letters* 34: L01303.
Yue LF, Suppe J, and Hung JH (2005) Structural geology of a classic thrust belt earthquake: The 1999 Chi-Chi earthquake Taiwan (M 7.6). *Journal of Structural Geology* 27: 2058–2083.
Zoback MD (2000) Strength of the San Andreas. *Nature* 405: 31–32.
Zoback MD, Barton CA, Brudy M, *et al.* (2003) Determination of stress orientation and magnitude in deep wells. *International Journal of Rock Mechanics* 40: 1049–1076.
Zoback MD and Beroza GC (1993) Evidence for near-frictionless faulting in the 1989 (M 6.9) Loma Prieta, California, earthquake and its aftershocks. *Geology* 21: 181–185.
Zoback MD and Healy JH (1984) Friction, faulting, and '*in situ*' stresses. *Annales Geophysicae* 2: 689–698.
Zoback MD and Healy JH (1992) *In situ* stress measurements to 3.5 km depth in the Cajon Pass Scientific Research Borehole: Implications for the mechanics of crustal faulting. *Journal of Geophysical Research* 97: 5039–5057.
Zoback MD, Zoback ML, Mount VS, *et al.* (1987) New evidence on the state of stress of the San Andreas fault system. *Science* 238: 1105–1111.